American Concrete Institute®
Advancing concrete knowledge

Committee 544
Fiber Reinforced Concrete

Agenda ACI 544-E
Mechanical Properties Sub-Committee Meeting,

Monday, March 24, 2014, 5 PM - 6:30 PM

Grand Sierra Resort,
Reno, NV

Room: Whitney

1. CALL TO ORDER and APPROVAL OF AGENDA
2. INTRODUCTIONS
3. ANNOUNCEMENTS
4. REVIEW OF THE NOMENCLATURE DOCUMENT
5. 544.FR - Report on Indirect Method to Obtain a Stress-Strain Diagram for Strain-Softening FRCs
   - Review of the latest TAC Comments
6. OTHER BUSINESS / PRESENTATIONS / INFORMAL DISCUSSION OF PROJECTS
7. ADJOURNMENT

ACI CT definitions

crack — a complete or incomplete separation, of either concrete or masonry, into two or more parts produced by breaking or fracturing. (See also **fracture**.)

crack, diagonal — in a flexural member, an inclined crack caused by shear stress, usually at about 45 degrees to the axis; or a crack in a slab, not parallel to either the lateral or longitudinal directions.

crack, hairline — a concrete surface crack with a width so small as to be barely perceptible.

crack, longitudinal — a crack that develops parallel to the length of a member.

crack, plastic-shrinkage — surface crack that occurs in concrete prior to initial set.

crack, shrinkage — crack due to restraint of shrinkage.

crack, transverse — a crack that crosses the longer dimension of the member.

crack-control reinforcement — see **reinforcement, crack control**.

cracked section — a section designed or analyzed on the assumption that concrete has no resistance to tensile stress.

cracking —

cracking, diagonal — development of diagonal cracks. (See also **tension, diagonal**.)

cracking, map —(1) intersecting cracks that extend below the surface of hardened concrete; caused by shrinkage of the drying surface concrete that is restrained by concrete at greater depths where either little or no shrinkage occurs; vary in width from fine and barely visible to open and well-defined; or (2) the chief symptom of chemical reaction between alkalies in cement and mineral constituents in aggregate within hardened concrete; due to differential rate of volume change in different portions of the concrete; cracking is usually random and on a fairly large scale, and in severe instances the cracks may reach a width of 0.50 in. (12.7 mm). (See also

cracking, **crazing**; also known as pattern cracking.)

cracking, pattern — see **cracks**, and **cracking, map**.

cracking, shrinkage — cracking of a structure or member due to failure in tension caused by external or internal restraints as reduction in moisture content develops, carbonation occurs, or both.

cracking, stress-corrosion — a cracking process that requires the simultaneous action of a corrodent and sustained tensile stress. (This excludes corrosion-reduced sections that fail by fast fracture; also excludes intercrystalline or transcrystalline corrosion that can disintegrate an alloy without either applied or residual stress).

cracking, temperature — cracking due to tensile failure, caused by temperature drop in members subjected to external restraints or by temperature differential in members subjected to internal restraints.

cracking load — see **load, cracking**.

cracks —

cracks, craze — fine random cracks or fissures in a surface of plaster, cement paste, mortar, or concrete.

cracks, D-line — see **D-cracks** (preferred term.)

cracks, pattern — see **cracks** and **cracking, map**.

craze cracks — see **cracks, craze**.

crazing — the development of craze cracks; the pattern of craze cracks existing in a surface. (See also **checking** and **cracks**.)

stiffening, early — the early development of an abnormal reduction in the working characteristics of a hydraulic cement paste, mortar, or concrete, which may be further described as false set, quick set, or flash set.

stiffening, premature — see **set, false** and **set, flash** (preferred term).

stiffness — resistance to deformation.

stiffness factor — see **factor, stiffness**.

strain — the change in length per unit of length, in a linear dimension of a body; a dimensionless quantity that may be measured conveniently in percent, in inches per inch, in millimeters per millimeters, but preferably in millionths.

strain, unit — deformation of a material expressed as the ratio of linear unit deformation to the distance within which that deformation occurs.

~~**strain** — the change in length per unit of length, in a linear dimension of a body; a dimensionless quantity that may be measured conveniently in percent, in inches per inch, in millimeters per millimeters, but preferably in millionths.~~

strength, flexural — the property of a material or a structural member that indicates its ability to resist failure in bending; in concrete flexural members, the stress at which a section reaches its maximum usable bending capacity; for under-reinforced concrete flexural members, the stress at which the compressive strain in the concrete reaches 0.003; for overreinforced concrete flexural members, the stress at which the compressive stress reaches 85 % of the cylinder strength of the concrete; for unreinforced-concrete members, the stress at which the concrete tensile strength reaches the modulus of rupture. (See also **modulus of rupture.**)

strength, nominal flexural — the flexural strength of a member or cross section calculated in accordance with provisions and assumptions of the strength-design method before application of any strength-reduction (Φ) factor.

strength, shear — the maximum shearing stress a flexural member can support at a specific location as controlled by the combined effects of shear forces and bending moment.

strength, specified compressive — compressive strength of concrete used in design.

strength, specified concrete compressive — the specified resistance of a concrete specimen to axial compressive loading used in design calculations and as a criterion for material proportioning and acceptance.

strength, specified concrete equivalent — in-place concrete compressive strength adjusted by correction factors that can be directly substituted into conventional strength equations with customary strength reduction factors.

strength, splitting tensile — tensile strength of concrete determined by a splitting tensile test.

strength, tensile — maximum unit stress that a material is capable of resisting under axial tensile loading; based on the cross-sectional area of the specimen before loading.

strength, transfer — the concrete strength required before stress is transferred from the stressing mechanism to the concrete.

strength, transverse — see **strength, flexural** and **modulus of rupture**.

strength, ultimate — an obsolete term; see

strength, nominal.

strength, yield — the stress at which a material exhibits a specific limiting deviation from the proportionality of stress to strain.

Previous ACI 544 Documents

Extracted from 5441R

The following FRC terms are not already defined in ACI 116R "Definitions of Terms for Concrete."

aspect ratio—the ratio of length to diameter of the fiber. Diameter may be equivalent diameter.

balling—when fibers entangle into large clumps or balls in a mixture.

bend-over-point (BOP)—The greatest stress that a material is capable of developing without any deviation from proportionality of stress to strain. This term is generally (but not always) used in the context of glass fiber reinforced concrete (GFRC) tensile testing. See "PEL" for flexural testing. The term "First Crack Strength" is the same property but often used for fiber concretes other than GFRC.

collated—fibers bundled together either by cross-linking or by chemical or mechanical means.

equivalent diameter—diameter of a circle with an area equal to the cross-sectional area of the fiber. See "SNFRC Terms" for the determination of equivalent diameter.

FIBER REINFORCED CONCRETE Definitions From 544.1R-5

fiber count—the number of fibers in a unit volume of concrete matrix.

first crack—the point on the flexural load-deflection or tensile load-extension curve at which the form of the curve first becomes nonlinear.

first crack strength—the stress corresponding to the load at "First Crack" (see above) for a fiber reinforced concrete composite in bending or tension.

flexural toughness—the area under the flexural loaddeflection curve obtained from a static test of a specimen up to a specified deflection. It is an indication of the energy absorption capability of a material.

impact strength—the total energy required to break a standard test specimen of a specified size under specified impact conditions.

modulus of rupture (MOR)—the greatest bending stress attained in a flexural strength test of a fiber reinforced concrete specimen. Although modulus of rupture is synonymous with matrix cracking for plain concrete specimens, this is not the case for fiber reinforced concrete specimens. See proportional elastic limit (PEL) for definition of cracking in fiber reinforced concrete.

monofilament—single filament fiber typically cylindrical in cross-section.

process fibers—fibers added to the concrete matrix as fillers or to facilitate a production process.

proportional elastic limit (PEL)—the greatest bending stress that a material is capable of developing without significant deviation from proportionality of stress to strain. This term is generally (but not always) used in the context of glass fiber reinforced concrete (GFRC) flexural testing. "Bend Over Point (BOP)" is the term given to the same property measured in a tensile test. The term "First Crack Strength" is the same property, but often used for fiber concretes other than GFRC.

specific surface—the total surface area of fibers in a unit volume of concrete matrix.

toughness indices—the numbers obtained by dividing the area under the load-deflection curve up to a specified deflection by the area under the load-deflection curve up to "First Crack."

ultimate tensile strength (UTS)—the greatest tensile stress attained in a tensile strength test of a fiber reinforced concrete specimen.

SFRC—steel fiber reinforced concrete.

embrittlement—loss of composite ductility after aging caused by the filling of the interstitial spaces surrounding individual glass fibers in a fiber bundle or strand with hydration products, thereby increasing fiber-to-matrix bond and disallowing fiber slip.

AR-GFRC—alkali resistant-glass fiber reinforced concrete.

GFRC—Glass fiber reinforced concrete. Typically, GFRC is AR-GFRC.

P-GFRC—polymer modified-glass fiber reinforced concrete.

polymer addition—less than 10 percent polymer solids by volume of total mix.
Polymer modified—Greater than or equal to 10 percent polymer solids by volume of total mix.

denier—weight in grams of 9000 meters of a single fiber

equivalent diameter—diameter of a circle with an area equal to the cross-sectional area of the fiber. For SNFRC, equivalent fiber diameter, d, is calculated by:
where:
f = 0.0120 for d in mm
f = 0.0005 for d in inches
D = fiber denier
SG = fiber specific gravity

fibrillated—a slit film fiber where sections of the fiber peel away, forming branching fibrils.

fibrillated networks—continuous networks of fiber, in which the individual fibers have branching fibrils.

monofilament—any single filament of a manufactured fiber, usually of a denier higher than 14. Instead of a group of filaments being extruded through a spinneret to form a yarn, monofilaments generally are spun individually.

multifilament—a yarn consisting of many continuous filaments or strands, as opposed to monofilament, which is one strand. Most textile filament yarns are multifilament.

post-mix denier—The average denier of fiber as dispersed throughout the concrete mixture (opened fibrils).

pre-mix denier—The average denier of fiber as added to the concrete mixture (unopened fibrils).

staple—cut lengths from filaments. Manufactured staple fibers are cut to a definite length. The term staple (fiber) is used in the textile industry to distinguish natural or cut length manufactured fibers from filament.

SNFRC—synthetic fiber reinforced concrete.

tenacity—having high tensile strength.

tow—A twisted multifilament strand suitable for conversion into staple fibers or sliver, or direct spinning into yarn.

NFRC—natural fiber reinforced concrete.

PNF—processed natural fibers

PNFRC—processed natural fiber reinforced concrete

UNF—unprocessed natural fibers

Crack initiation- The start of a crack in a member at a point where stresses are concentrated due to the release of energy contained within the stressed member in terms of strain energy. (*For a stressed sample, when the strain energy available at the vicinity of a flaw or notch is sufficiently high to match the fracture toughness, energy is released and cracks are initiated.*)

Stable Crack Propagation –The incremental and sequential growth of a crack through external energy input as in increase in the load magnitude. *(The crack propagation requires and consumes a steady supply of energy. If the only source of available or additional energy is supplied through an increase in the load level, then crack propagation can be incremental and dependent on increasing the load on the specimen. This incremental and sequential growth of crack is defined as stable crack propagation.)*

Unstable Crack Propagation - The instantaneous uncontrollable and dynamic crack propagation of an existing crack due to release of energy contained within the stressed body or the loading system in terms of strain energy. An increase in the load level is not required to initiate the uncontrollable crack propagation. *(also see stable crack propagation, The crack propagation requires and consumes a steady supply of energy. If the source of available energy is through the strain energy that is already stored in the sample or the loading system, an increase in the load is not required for the crack growth; consequently the crack can extend even though the load on the specimen decreases. This type of crack growth occurs suddenly and instantaneously and is defined as unstable crack extension or unstable crack propagation.)*

Crack Width- crack opening under applied load, *(Opening of the crack as a function of degree of interlock and applied loads transferred through the crack)*

Microcracking –The formation of localized, microscopic cracks within concrete of the order to about 0.1 mm wide and up to a few mm long. *(The microcracks may not be detectable by naked eye. Therefore the primary definitions used by ACI on crack detection are not applicable.)*

Limit of Proportionality (LOP) *(See limit of proportionality)*

Bend over Point (BOP)- First crack strength of a fiber reinforced concrete sample under uniaxial tension. *(First crack strength of a fiber reinforced concrete sample under uniaxial tension.)*

Localization- The state where an imposed deformation on a sufficiently large and uniform member translates into the opening of a single crack, described as the critical failure crack. The rest of the sample may experience a uniform state of strain or reduce its strain as the crack widens. *(The process where the apparent strain distribution along the length of a specimen even under a uniaxial tension condition is non-uniform and depends on the opening within cracked regions and an n average strain in the un-cracked regions.)*

Ultimate Tensile Strength (UTS)- Ultimate tensile strength of a fiber reinforced concrete sample under uniaxial tension. *(Ultimate tensile strength of a fiber reinforced concrete sample under uniaxial tension expressed as a nominal stress.)*

Strain Softening (I) – A process of decreasing stress as nominal strain increases, where unstable crack propagation directly follows crack initiation, or after the ultimate strength has reached. *(Plain concrete is strain-softening and may be quasi- brittle or brittle depending on strength. As soon as the unstable cracking occurs, the sample loses its ability to carry additional load carrying capacity and it follows through a descending branch in load capacity.)*

Strain Softening (II)– Fiber reinforced concrete composite with a primarily linear elastic ascending tensile stress-strain curve up to a point representing both the first cracking (BOP) and peak stress (UTS). Response is followed by a decrease in resistance and localized cracking, where all subsequent stresses remain smaller than the first cracking (maximum) stress.

Strain Softening Fiber Reinforced Cement (or concrete) **(SS-FRC)** *(See strain softening)*

Strain Hardening (I)- A process where stable crack propagation directly follows crack initiation. *(Increasing stress with increasing strain, though at a rate much lower than the young's modulus and at a decreasing rate)*

Strain Hardening (II) - Fiber reinforced concrete composite with a primarily linear elastic ascending tensile stress-strain curve up to first cracking (BOP), and a post-elastic portion characterized by an increase in the stress with a much lower effective stiffness, (representing tension stiffening) up to the maximum stress (UTS). *(The first cracking and peak stress points are distinctly different. Response between the first cracking stress and peak stress is gradual with a stiffness that is lower than the uncracked stiffness. Response after the peak stress is strain softening)*

Strain Hardening Fiber Reinforced Cement (or concrete) (**SH-FRC**) *(See Strain Hardening)*

Deflection Softening –Fiber reinforced concrete composite with a load-deflection curve in bending that shows a primarily linear elastic ascending branch up to first cracking, followed by immediate reduction in load with an increasing deflection where all subsequent loads remain smaller than the first cracking load. *(In principle, deflection softening also occurs in plain concrete when we conduct the test under controlled crack opening mode and measure the stress crack opening response at the fine scale. Deflection softening in plain concrete is characterized by a brittle fracture like response.)*

Deflection Softening Fiber Reinforced Cement (or concrete) (**DS-FRC**) *(See Deflection Softening)*

Deflection Hardening - Fiber reinforced concrete composite with a load-deflection curve in bending that shows an initial elastic portion to first cracking, followed by a post-elastic portion that is either horizontal or ascending leading to the maximum flexural load that is used to obtain an equivalent modulus of rupture or bending strength. *(The end of the initial ascending portion of the curve is followed by a significant decrease in stiffness, which is indicative of the first flexural cracking. The maximum load or peak load and corresponding deflection are significantly larger than the load and deflection at the first flexural cracking.)*

MOR- Modulus of Rupture

(flexural strength (obtained from the maximum load resistance) computed using linear elastic equation for stress distribution in a flexural specimen. Also referred to as modulus of rupture.)

Deflection Hardening Fiber Reinforced Cement (or concrete) (**DH-FRC**) *(See deflection hardening)*

Addition suggestions

Alkali resistivity

alkali attack

chemical attack ;

fiber content

Engineered cementitious composites

fiber length

fiber orientation

First crack strength ;

frictional bond

length distribution of fibers

Plastic viscosity

rheology

surface treatments

impact velocity

Absorption

accelerated ageing tests;

accelerated ageing; ageing mechanisms

Accelerated aging

Accelerators

ACK model see Aveston Cooper and Kelly model

Acrylic fibers

Adhesional shear bond strength

adhesional strength

Anchorage

AR glass fibers see Glass fibers

Aramid fibers

Asbestos

Asbestos cement

Aspect ratio

Aveston Cooper and Kelly model

Axial behavior

Backcalculation procedures

Bamboo fibers

Beam specimens

Beam-column connection

Beam-column stiffness degradation

Beam-test, 4 point bending, 3 point bending

Bend over point

Bending

Biaxial loading

biological attack; carbonation ; dimensional changes;

Blast loading ;

Bond

Bond failure

Bond-slip relationship

Bond splitting

Bond strength

Bond strength and toughness ; elastic modulus ; other variables

Bond stress distribution

Bond stresses

Bond tests

bonding; interfacial transition zone

BOP

Bridging force

brittleness ratio

Bundled fibers;

Cable

Calcium sulpho-aluminate cements

Capacity

Carbon

Carbon fiber reinforced concrete:

Carbon fibers,

Carbonation;

Cellular concretes

Cellulose fibers

Cellulose pulp reinforcement-;

Cementitious composites

CemFil- glass fibers

CFRP sheet

Characteristic stress values;

Charpy test

chemical attack fiber-matrix bond microstructural mechanisms;

chemical composition

chloride attack ;

cladding

Cladding

closed loop control

Coefficient of friction

Column

Compact reinforced composite

compaction pressure; compressive strength;

compliance

Composite beams

Composite connections

composite materials approach

Composite stiffness

Composite structures

composite with continuous and aligned fibers ;

composition durability

composition; moisture content;

compression members ;

Compression Molding

Compressive strength

Compressive toughness

Concrete columns

Concrete deterioration

concrete primary

Concrete slabs

Confined concrete

Confinement

Connection behavior

Connection restraint

Connections

Contamination

content ; fiber orientation

continuous hand laid reinforcement- short randomly mixed fibers;

Continuous production process

Continuous reinforcement;

conventional high performance ;

Cook-Gordon arrest mechanism

Corrosion

Corrosion resistance

Cost-benefit analysis

Cotton fibers

Coupling agents

Coupon testing

Cover splitting

Crack

Crack bridging

crack control;

Crack mouth opening displacement

crack opening curve; crack stabilization;

Crack repair

Crack spacing

crack suppression;

crack width ;

Crack width and spacing

crack-fiber interactions;

Cracking

creep

crimped fibers; deformed fibers

critical fiber content

Critical fiber length

critical fiber length ; curing ; dimensional stability; durability; electrical resistivity ; failure mechanism ;

critical fiber volume

critical strain energy release rate

critical stress intensity factor

Curing

Curvature

Cyclic loading

Cylinder compression test

Cylindrical

Damage

Damage Parameter

Debonding

debonding (frictional) energy ;

Deck

Deck panels

Defects

Deflection

deflection hardening

deflection softening

Deformation

deformed ; distribution

Deformed fibers

degradation; properties

degree of refinement

Delamination

Denier unit ; relationship with fiber diameter

Densified small particle systems (DSP)

Density (mass/volume)

design considerations

Design guidelines

Differential scanning calorimetry

Diffusion

dimensional changes

Direct shear

direction of casting

Discrete laminated plates

distribution and

distribution of stresses; elastic

Dowel

Dredging

drop-weight

Drying shrinkage

drying shrinkage ; fiber

drying/wetting cycles ;

Ductile

Ductility

Durability

durability AR fibers-

Durability testing; accelerated tests; drying/wetting ; natural exposure

Dynamic Characterization

Dynamic Loading Devices

Dynamic response

dynamic test

Dynamic Testing

Earthquake

ECC

effect on first crack stress ; relationship with fiber diameter;

Effective moment of inertia

efficiency factor

Efficiency of fiber reinforcement

E-glass

E-glass ageing

Elastic modulus

Elastic shear stress

elastic-plastic

Elastomers

electrical measurements

Embedment

Embedment length

Energy absorption

energy balance;

energy criterion;

energy increase;

Engineered cementitious composites

Engineering properties

Environment

environmental effects

Environmental performance

Epoxy

Epoxy bonded plate

error signal

Explicit Analysis

Exposure

expression for cylindrical fibers ;

Extraneous deflections;

Extrusion

extrusion-; properties

Fabric

fabric bonding

fabrics spacer

Failure

Failure mechanisms

Failure modes

Fastener

Fatigue

Fatigue stiffness

Fatigue-life

Fatigue-test

FEM-calculation

FE-method

Ferrocement

Fiber bending effect on orientation efficiency

Fiber cement interactions; curing effects;

fiber constitutive response ;

Fiber content:

Fiber count and surface area

Fiber debonding

fiber degradation ; physical interactions ;

fiber dimensions

fiber embrittlement

fiber mats;

Fiber orientation; effect on efficiency constant fiber angle

Fiber packing

Fiber properties

Fiber pull-out

Fiber reinforced cementitious materials applications;

Fiber reinforced concretes

Fiber spacing:

Fiber tensile stress equations

Fiber-architecture

Fiberboard

Fiber-matrix interface

Fibers primary reinforcement

Fibers secondary reinforcement

Fibers versus welded wire mesh

fibers versus welded wire mesh;

Fibers, Polyvinyl alcohol PVA fibers

fictitious crack model;

Fill Yarns

finishing ;

Finite element analysis

Finite element modeling

Fire resistance

First crack strain

First crack stress

Flexibility

Flexural behavior

Flexural behavior modeling

Flexural capacity

Flexural design

flexural design procedures;

Flexural impact toughness

flexural properties

flexural properties local stresses ;

Flexural stiffness

flexural strength ;

flexural strength retention

Flexural tests

flexural toughness

Flexure

Fly ash

Fly ash reduction in alkalinity

Flyash

force transfer

force-displacement curve

forces

Formwork (construction)

fracture energy

fracture energy load-deflection curve

Fracture mechanics

Fracture properties

fracture toughness

Freeze thaw durability

freeze-thaw

Frequency

Fresh concretes

fresh mix tests;

fresh properties

frictional bond ;

Frictional shear strength

Frictional shear stress

frictional slip

frictional stress transfer;

Full-scale prototype test

Gage length

Geomaterials

Geometry structure of interface

geometry of fiber crossing a crack

Geosynthetics

Geotextiles

GFRC

Glass

Glass fiber

Glass fiber reinforced cement;

glass fibers

Glass fibers ; alkali resistant (AR)

Grid

Grid architecture

Griffith equation

Griffith equation ;

Hand layup

hardened concrete tests

hardened properties

Hatschek process:

heat-rain tests ;

high density matrices

high loading rates ;

high modulus; low modulus; properties ;

High performance systems;

High speed tension toughness

high strain rates;

High strength concretes

high strength matrix

High-rise building

Highways

Honeycomb

Hybrid fiber systems

Hybrid rebar

Hydraulic cements

Hygrothermal aging

Hygrothermal stability

Impact

impact loading

Impact resistance ;

Impact strength

Impact testing;

Impact tests

impact toughness ;

Implicit Analysis

Indentation

inelastic curvature

inertial effects;

In-plane shear stiffness

Installing

interactions with steel fibers ; smeared crack model ;

Interface

interfaces and bond;

Interfacial frictional bond strength

interfacial shear

interfacial shear strength ;

Interfacial transition zone

Interfacial transition zone (lTZ)

interpretation of curves ;

Inverse Analysis

ITZ

Joint

Joints (junctions)

Jute fibers ; properties ;

Kevlar

kraft process-

Lamina

Laminate

Layered system

Lightweight concrete

linear elastic fracture mechanics (LEFM)

Load deflection curves ;

Load testing

Load-deflection curve

Localization

Long term behavior

Magnani process

Matrix

maximum bending load

maximum load

maximum load versus fiber displacement; modeling and analysis;

Mechanical properties

mechanical properties long term ;

Mechanical testing

mechanics and microstructure

mechanics- critical fiber volume

mechanics- modeling

mechanics- modeling

mechanics of the composite materials

mechanics of the composite materials;

Metal fibers

Microcracking

microfibers ;

microhardness ;

Microhardness of fibers

Microindentation tests

Micromechanics

modeling of flexural behavior

modeling of tensile behavior

modulus of elasticity ;

Modulus of Rupture

Moment redistribution

Moment-curvature

Moment-curvature relationship

Moments

monofilament fibers

multiple cracking;

Natural fibers

natural weathering

Nondestructive evaluation

normal stress

Nylon fibers

One-way slabs

Fiber orientation and distribution

orientation effects

Overlay

PAN (polyacrylonitrile) fibers;

Passive confinement

Patch

pavements and slabs on grade

Performance tests

Permeability

Physical properties

Pile

Pipes (tubes)

pitch carbon fibers;

Placing

placing ; production technologies

Plain concrete

plain versus fiber reinforced concrete;

Plastic deformation of fibers

Plastic Hinge

Plastic shrinkage

Plastic shrinkage and cracking tests

Plasticity

Plate

Plate bonding

Plate load tests

Plates(structural members)

Poisson effect

Polyacrylonitrile (PAN) fibers

Polyester fibers

Polyethylene fibers;

Polyethylene terephthalate (PET)

Polyimides

Polymer

Polymer matrix

Polymer-cement matrices

polymer-portland cement matrices

Polypropylene fiber

Polyvinyl alcohol (PVA) fibers-

Post-buckling behavior

pozzolanic fillers;

Premix process

Prestressed concrete

Pre-tension

Process Zone

production curing, pre-mixing

Production methods

production processes; replacement by other fibers;

production technologies;

projectile impact ; repeated impact tests;

properties ; pull-out work

properties effect on strength

properties specifications and tests

properties and behaviour

properties fiber efficiency fiber

properties of fibers ;

properties; "telescope" failure sleeve-core failure;

Protective coatings

Public works

Pullout

pull-out behavior;

pull-out of fibers; reinforcing mechanisms bonding and

Pull-out see Fiber pull-out

Pullout test

pull-out: analysis cracked composites

Pulp

Pulp type processes

Pultruded

Pultrusion

PVA

Quality assurance

Quality control

Random-fiber

range of proportions ;

Rapid set cement

Ratio

R-Curve

Reactive powder concrete (RPC)

reinforcement secondary

reinforcement;

Reinforcing materials

Relaxation

Repair

Residual strength

Resistance Curves

resistivity; high tenacity

restrained ; ring test

restrained shrinkage

Restraints

Retrofit

reversed cyclic loading ;

Rigid pavement

rigidity of impact machine

Roller

Rule of mixtures

Sandwich structures

Scale effects

Seismic applications

Seismic retrofit

Seismic upgrade

seismic; self-compacting FRC;

Self-compacting FRC

self-consistent methods

Semi-rigid

Service condition

shear and torsion; shotcrete

Shear capacity

Shear deformation

Shear failure

Shear lag theory

Shear properties

Shear strength

shear strength design;

shear stresses;

shear transfer

Shell

Shotcrete

Shrinkage

shrinkage cracking

Shrinkage of hardened FRC

Shrinkage Ring test

shrinkage thermal effects

SIFCON

SIFCON see Slurry infiltrated fiber concrete

silica fume

SIMCON see Slurry infiltrated mat concrete

single fiber ; stress transfer in cracked

Sisal fibers

Site characterization

Sizing

Slab

Slenderness

Slip

Slip hardening

slip hardening fibers

Slip modulus

Slip softening

Slow crack growth

Slump

Slump test

Slurries

Slurry infiltrated fiber concrete

Spacing factor

specific work of fracture;

specimen size

Spin casting

split Hopkinson pressure bar;

Splitting tensile strength

spray-up;

Standards

Static loads

static versus impact tests ;

static; mix design

Steel fiber mat

Steel fiber reinforced concrete:

Steel fibers:

Stiffness

stiffness degradation

Stirrups

Strain

strain at termination ;

strain distribution

Strain energy release rate

Strain hardening

Strain softening

Strains

Strength

strength equations;

strength in pull-out;

Strengthening

stress in a fiber crossing a crack

Stress intensity Factor

stress transfer

Stress-crack width relationship

Stresses

Stress-rupture

stress-strain

stress-strain curve

stress-strain curve; thin sheet

stress-strain curves ;

Stress-strain diagram

Stress-strain relationship

structural analysis

Structural characterization

Structural design

structural design considerations

Structural design considerations for FRC

Structural performance evaluation

Structural shapes

structural use

structure and properties

structure of bulk matrix ;

structure; temperature effects ; tensile creep ; yarns

Styrene

Subgrades

Sugarcane (bagasse) fibers

surface area after milling ; tensile strength

surface treatments-;

Survey

Sustainability

Synthetic fibers

Temperature

temperature effects

temperature extremes;

tensile behavior ;

Tensile capacity

Tensile strength

tensile strength splitting

Tensile stress

Tension

tension members

Tension stiffening

Tension test

test methods: fresh mix hardened composite;

Textile

Textile Architecture

Textile reinforced concrete

Thermal stress

thin sheet applications

thin-walled products;

Torex fibers

total energy

toughness

Toughness factor

Toughness index

Toughness tests

fracture mechanics

Triaxial loading

Tunnel lining

Tunnels

Ultimate condition

Ultimate load

Ultimate strength

Ultimate tensile strength

Uniaxial model

Unidirectional carbon fiber

vacuum dewatering

Viscosity

Void

volume changes

volume stability

Wall effect

Warp Yarns

Weathering

Welded wire fabric, Welded Wire Mesh (WWM)

Wetting and drying tests

wood (cellulose) ;

Wood fibers

Work of fracture

Workability

Workability tests

woven mat

yarn

yarns structure and properties

Zirconium

ACI 544.FR
To TAC

Report on Indirect Method to Obtain a Stress-Strain Diagram for Strain-Softening Fiber-Reinforced Concretes (FRCs)

Reported by ACI Committee 544

Barzin Mobasher*	Neven Krstulovic-Opara*†	Clifford N. MacDonald
Chair	Secretary	Membership Secretary

Corina-Maria Aldea
Emmanuel K. Attiogbe
Nemkumar Banthia
Joaquim Oliveira Barros*
Gordon B. Batson
Peter H. Bischoff
Jean-Philippe Charron
Xavier Destree
Ashish Dubey
Mahmut Ekenel
Liberato Ferrara
Gregor D. Fischer
Dean P. Forgeron
Antonio Gallovich
Rishi Gupta
George C. Hoff
John Jones
David A. Lange
Maria E. Lopez de Murphy
Michael A. Mahoney
Bruno Massicotte
Christian Meyer
James Milligan
Nicholas C. Mitchell, Jr.
Gerald H. Morton
Antoine E. Naaman*
Jeffrey L. Novak
Giovanni A. Plizzari
Max L. Porter
Venkataswamy Ramakrishnan
Klaus Alexander Rieder
Pierre Rossi
Surendra P. Shah
Flavio de Andrade Silva
Kay Wille
Carla V. Yland
Robert C. Zellers
Lihe Zhang

*Members of the subcommittee who authored this report.
†Chair of the subcommittee that drafted this report.

This report presents existing methods for estimating uniaxial tensile stress-strain response of strain-softening fiber-reinforced concretes (FRCs) from flexural beam-test data using an approach originally developed by RILEM (2003) and later modified through British Standard BS EN 14651:2005+A1:2007 (British Standards Institution 2007). Different approaches based on curve fitting or back-calculation of flexural data can be used to compute tensile response. Two of these approaches applied to beam tests are the empirical and inverse analysis methods, which are used for obtaining the uniaxial tension stress-strain values needed for design. These two approaches are presented in detail. Results for a range of FRC materials studied show the back-calculated post peak residual tensile strength is about 30 to 37 percent of the elastically equivalent flexural residual strength for specimens with different fiber types and volume fractions.

Keywords: fiber-reinforced concrete; inverse analysis; tensile stress-strain diagram.

CONTENTS

CHAPTER 1—INTRODUCTION AND SCOPE

1.1—Introduction

This report provides guidelines for obtaining uniaxial stress-strain curves of strain-softening fiber-reinforced concretes (FRCs) from beam test data.

To develop and apply design procedures for FRC materials, simplified equations are needed to account for fiber's contribution to the tensile response, especially after cracking has occurred. A majority of FRC mixtures exhibit tensile strain-softening response, which is associated with the role that fibers play in bridging a main tensile crack, thus resisting its opening and generating a force. The force-resisting crack opening, also referred to as bridging force, is represented as an average effective stress and described by a tensile stress-crack width relationship. This report addresses methods to compute the stress transfer after cracking is initiated in a concrete section.

1.2—Scope

This report presents existing methods for estimating characteristic tensile stress-strain or tensile stress crack–width response of strain-softening FRCs using flexural beam test data. Methods are valid for the strain-softening FRCs that do not exhibit distributed or parallel micro-cracking when tested in flexural loading conditions.

A model for equivalent stress-strain diagram (Naaman and Reinhardt 2005; Noghabai 1998) is presented first and followed by calculation procedures for obtaining flexural tensile and residual flexural strengths from beam test data. The relationship is presented in terms of parameterised stress coefficients that are determined using a step-by-step inverse analysis procedure in Appendix A. The statistical aspects of back-calculated test data, however, are not addressed. Specific coefficient values provided for notched (RILEM (2003) and third-point beams (Belgian standard NBN B15-238-92) are validated. Since the coefficient values are not directly reported for beam types tested per ASTM C1609 and ASTM C1399, this report proposes an approach to do so and compares the results with other methods. The report concludes with the relationship between the parameters that define the stress-strain diagram and the experimental flexural residual strengths obtained.

CHAPTER 2—NOTATION AND DEFINITIONS

2.1—Notation

b = beam width

d = beam depth

E = Young's modulus

f_c' = uniaxial ultimate compressive strength

f_{eq} = equivalent flexural tensile strength parameter

f_R = residual flexural tensile strength parameter

F = force component in stress diagram

k = neutral axis depth ratio

L = clear span

L_f = fiber length

L_p = plastic length for crack localization in beams, in.

M = moment, in.-lb

M_{cr} = moment at first cracking, in.-lb

M_e = moment in elastic range, in.-lb

M_{it} = moment at an intersection point, in.-lb

M_u = ultimate moment, in.-lb

P_{cr} = total load at first cracking, lb

Vf = volume fraction of fiber

α = normalized transitional strain (ε_{trn} /ε_{cr})

β_{crit} = normalized critical tensile strain

β_{tu} = normalized ultimate tensile strain (ε_{tu} /ε_{cr})

δ_u = deflection at ultimate moment, in.

ε_c = compressive strain

ε_{cr} = first cracking tensile strain

ε_{cu} = ultimate compressive strain

ε_{cy} = compressive strain at yielding

$\underline{\varepsilon_t}$ = tensile strain

ε_{trn} = transitional tensile strain ($\alpha * \varepsilon_{cr}$);

ε_{tu} = ultimate tensile strain

λ = normalized top compressive strain ($\varepsilon_c / \varepsilon_{cr}$)

λ_{cu} = normalized top ultimate compressive strain ($\varepsilon_{cu} / \varepsilon_{cr}$);

λ_{tu} = normalized top compressive strain when bottom fiber reaches ultimate tensile strain

μ = normalized postpeak tensile strength

μ_{crit} = critical normalized postpeak tensile strength to make elastic perfectly plastic moment-curvature diagram

σ_c = compressive stress, psi

σ_{cy} = compressive yield stress, psi

σt = tensile stress, psi

φ = curvature

φ_{cr} = curvature at first cracking

φ_{it} = curvature at an intersection point

φ_u = ultimate curvature

ω = compressive to tensile strength ratio ($\varepsilon_{cy}E/\varepsilon_{cr}E$)

2.2—Definitions

ACI provides a comprehensive list of definitions through an online resource, "http://www.concrete.org/Tools/ConcreteTerminology.aspx." Definitions provided here complement that source.

bend over point (BOP)—the maximum tensile stress that a material can develop without any deviation from proportionality of stress to strain. This term is generally used in the context of strain hardening cement composites. Refer to "proportional elastic limit (PEL)" for flexural testing and "first crack strength" which is also used for the same property.

crack bridging—the ability of fibers to extend from one face of a crack to the opposite side and transfer load during crack opening.

crack initiation—when the strain energy available for release at the vicinity of a flaw or notch is sufficient to match the fracture toughness, energy is released and cracks are initiated.

crack mouth opening displacement (CMOD) —measure of crack length extension beyond the tip of a notch created at the center of a beam specimen subjected to flexural loads in a three-point bending configuration.

crack widening—the opening of an existing crack expressed in units of length under the dual and opposing actions of external load and resistance offered by the fibers that provide crack bridging.

deflection hardening fiber-reinforced cement (or concrete) (**DH-FRC**)**—**Fiber-reinforced cement composite with a load-deflection curve in bending that shows an initial elastic portion up to the first flexural cracking, the limit of proportionality (LOP), followed by a post-elastic portion that is either horizontal or ascending leading to the maximum flexural load.

deflection softening fiber-reinforced cement (or concrete) (**DS-FRC**)**—**Fiber-reinforced cement composite with a load-deflection curve in bending that shows a primarily linear elastic ascending branch up to the first flexural cracking (LOP), followed by immediate reduction in load with an increasing deflection where all subsequent loads remain smaller than the first cracking load.

first crack—the point on the flexural load-deflection or tensile load-extension curve at which the form of the curve first becomes nonlinear.

first crack strength—the stress corresponding to the load at first crack for a fiber-reinforced concrete composite in bending or tension.

first flexural cracking (LOP)—if the maximum internal moment generated due to imposed flexural loads exceeds the cracking moment of the material, occurrence of first flexural cracks in the beam can be observed. Beyond this, load-deflection response of the material shows nonlinearity.

flexural tensile strength—is the fictitious stress acting at the tip of notch drawn at the center of a beam specimen subjected to flexural loads in a three-point bending test.

flexural toughness—the area under the flexural load-deflection curve obtained from a static test of a specimen up to a specified deflection, which is an indication of the energy absorption capability of a material.

microcracking—formation of localized, microscopic cracks within concrete, approximately 0.1 mm wide to a few mm that may not be visible.

modulus of rupture (MOR)—the greatest bending stress attained in a flexural strength test of a fiber-reinforced concrete specimen. Modulus of rupture is synonymous with matrix cracking for plain concrete specimens, but does not apply to fiber-reinforced concrete specimens. Refer to proportional elastic limit (PEL) for definition of cracking in fiber-reinforced concrete.

peak stress—computed using the peak load, it is the maximum stress that the material or structural element can sustain during a test.

proportional elastic limit (PEL)—the greatest bending stress that a material is capable of developing without significant deviation from proportionality of stress to strain, generally used in context with strain hardening cement composites under flexural testing. “Bend over point (BOP)” is used for the same property measured in a tensile test and “first crack strength” for general fiber concretes.

residual strength—the strength in the post-peak load region of a static load-deflection curve, calculated by dividing maximum bending moment along the specimen axis in the post-cracking stage at different deflection levels by the section modulus of original section.

serviceability limit state (SLS)—the performance criterion for serviceability of a structure, corresponding to conditions beyond which the structure might fail to meet technical requirements

such as stress limits, deformation limits, and crack control and, therefore, declared unfit for routine loading conditions.

smeared crack—formation of multiple cracks spread over a distinct area.

stable crack propagation—after a crack has initiated, its propagation requires and consumes energy. If the only source of additional energy is supplied through an increase in the load level, then crack propagation can be incremental and totally dependent to the additional load on the specimen. This incremental and sequential growth of crack is defined as stable crack propagation.

strain hardening fiber-reinforced cement (or concrete) (SH-FRC) **—**Fiber-reinforced cement composite with a primarily linear elastic ascending tensile stress-strain curve up to the first cracking bend over point (BOP), microcrack coalescence, and a post-elastic portion characterized by an increase in the stress with a much lower effective stiffness (representing tension stiffening), up to the maximum stress ultimate tensile strength (UTS). The two points of first cracking and peak stress are distinctly different. Response after the peak stress is followed by gradual unloading.

strain-softening fiber-reinforced cement (or concrete) (SS-FRC) —Fiber-reinforced cement composite with a primarily linear elastic ascending tensile stress-strain curve up to the same point representing both the first cracking bend over point (BOP) and also peak stress ultimate

tensile strength (UTS). Response is followed by unloading due to unstable cracking, where all subsequent stresses remain smaller than the first cracking (maximum) stress.

ultimate limit state (ULS) —is a design criterion and a purely elastic condition. It is a recommended state of stress within which the structure will behave in the same way under repetitive loading. A structure is deemed to satisfy the ULS criterion if all factored bending, shear and tensile or compressive stresses (or loads) are below the factored resistances calculated for the section under consideration.

ultimate tensile strength (UTS)—the greatest tensile stress attained in a tensile strength test of a fiber-reinforced concrete specimen.

unstable crack propagation—after a crack has initiated, its propagation requires energy consumption. If the source of energy is already contained within the stressed body in the form of strain energy, then the sample can unload and release the energy back into the crack, causing it to propagate uncontrollably and in a dynamic manner. An increase in the load level is not required and the crack propagation is instantaneous.

unstable cracking—the process by which microcracks grow sufficiently to join together and form a larger perhaps visible macrocrack that propagates through the entire section.

CHAPTER 3—TEST ANALYSIS

3.1—Strain softening and hardening

Strain softening is a process where formation of a crack under load is directly followed by its sudden and self-driven propagation. This occurs when the material is quasi-brittle with low bridging stress; upon cracking the sample loses its ability to carry load and the stress-strain response goes through a descending branch (Fig. 3.1). In Fig. 3.1 the post-cracking stress remains below the peak stress in subsequent loading (Namman and Reinhardt 1995). The softening behavior does not affect tensile strength, but increases tensile ductility and has a significant impact on the flexural load-carrying behavior.

If fiber content and bond are sufficiently high, the load-carrying capacity in tension exceeds the matrix cracking strength, a behavior referred to as strain hardening. In this process, stable crack propagation directly follows crack formation and the material could behave as perfectly plastic or exhibit hardening behavior. Since the sample is capable of supporting additional load, multiple parallel cracks are formed and the flexural load deformation response is also characterized by an ascending stress-strain branch up to the formation of a macro-crack or damage localization (Fig. 3.1).

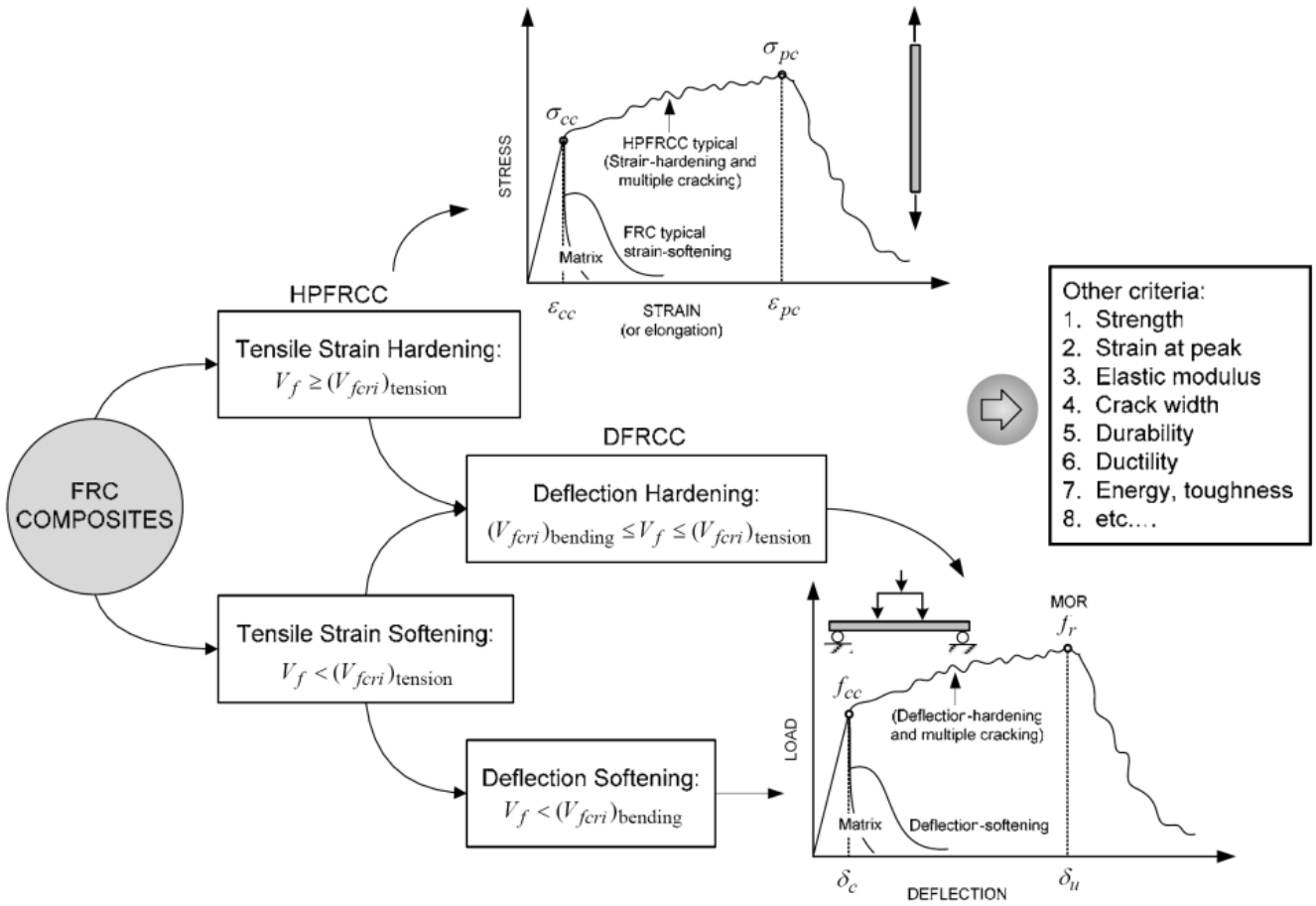

Fig. 3.1— Classification of fiber-reinforced concretes (FRCs) based on their tensile response (Naaman and Reinhardt 2005).

3.2—Deflection softening and hardening

Many of the physical, durability, and mechanical properties of fiber reinforced concrete (FRC) are affected by the amount, type, bond, and nature of anchorage of fibers used. For example, if the volume of the fibers in increased being a level designated as critical fiber content, then the entire stress strain response is also affected since the manner of load and strain distribution change in the sample. This is because as the plain matrix cracks, there are sufficient fibers to carry the load that is being released by the matrix. Other criteria that are affected by the stress-strain response include, but are not limited to strength, strain capacity, first crack strain, elastic

modulus, crack width, durability, permeability, total energy absorption, fatigue life, thermal conductivity, and shrinkage and creep characteristics.

Since the flexural design of FRC elements is generally governed by the tensile stress-strain response of the material, the post-cracking behavior in terms of strain softening or hardening has a direct effect on the results (Soranakom and Mobasher 2009b). Proper characterization of the load-deformation response and computation of valid material behavior data from these tests is essential to successful design applications (Banthia and Trottier 1995a, b; Mobasher 2011; Cunha 2010).

Fiber-reinforced concrete materials have been extensively studied under direct tension loading conditions. Technical problems exist in conducting stable tests to obtain strain-softening response that include:

a) Inherent instability of crack propagation from one side of the specimen to the other that changes the uniformity of applied deformation;

b) Difficulty in control algorithm due to brittleness of the composite;

c) Test results that are significantly influenced by the support boundary conditions of fixed or free, specimen size, and notched versus unnotched specimens (Van Mier 1996);

d) Maintaining objectivity in the closed loop control conditions, such as cracking symmetry for notched specimens (Mobasher 2011; Hordijk 1991).

One method to calculate post-cracking behavior is to use the experimental flexural results and reduce them into a set of material parameters that are in compliance with the model assumptions.

Flexural behavior may vary significantly depending on whether FRCs exhibit strain-softening or -hardening response. An approach to classify FRC based on its tensile mechanical response from the uniaxial tension can also be extended to flexural behavior. This classification depends on the efficiency and amount of fibers that covers a range from strain softening to hardening (Naaman and Reinhardt 2005).

The difference between the tension and flexural test results of strain-softening materials is that in a tension test, the post-peak tensile stress-crack width response does not influence the maximum load obtained. In a flexural test, the maximum load can be directly related to the softening stress levels such that the overall behavior changes to an ascending post-cracking response, which is defined as deflection hardening. While a strain-softening FRC can develop deflection softening or deflection hardening based on the residual stress level present, FRC with tensile strain-hardening behavior always exhibits a deflection hardening response.

Many structural systems with strain-softening materials, such as structural floors or indeterminate structures, can exhibit deflection-hardening behavior and an increase in ultimate strength values in proportion to the residual strength. While the tension test theoretically shows the true material behavior and flexural test represents a structural response, a flexural test is often used as a means of property measurement.

3.3—Equivalent tensile stress-strain responses

An alternative approach to direct measurement of the stress strain through uniaxial tension test is to consider flexural tests data since these tests are often used in quality control. Back-calculation of equivalent tension results from flexural tests, defined as inverse analysis, can be a valid compromise since many researchers use these tests to obtain the equivalent tension response needed in member design. Approaches have been developed by RILEM (2003) and European Standard CSN EN 14561 (2007). The equivalent tensile response can then be used in the design of flexural members for applications such as slabs, panels, and other applications where fiber contribution can be estimated with equivalent softening parameters. Different approaches do not always yield unique results, as assumptions regarding the shape of the stress-strain response inherently affect the back-calculated parameters and, therefore, several test methods for calculation of the equivalent tensile properties are summarized. An overview of the existing inverse methods for obtaining uniaxial tensile stress-strain curves from beam test data follows (3.4).

3.4—Inverse analysis methods

There is no standard specimen geometry for flexural testing. RILEM (2003), CEB-FIBP Model Code (MC) 2010 (2011), and CSN EN 14651 (2007) approaches use notched three-point bending tests loaded along the midspan of a notched beam. ASTM methods, however, recommend unnotched four-point beam tests. Based on these recommended standards, tensile stress-strain response can be calculated using prescribed parametric equations. Values of the coefficients of these equations are determined from the experimental data using an equivalent elastic or inelastic

method. The inverse-analysis method is optimal for finding values when specific coefficient values are unknown. Various inverse analysis approaches have been reported including:

a) Technical guidelines for FRC, developed by RILEM (2003) for steel fiber-reinforced concrete (SFRC) by introducing the concept of equivalent f_{eq} and residual f_R flexural tensile strength parameters. These values were used to derive the stress-strain or the stress-crack width response of a SFRC (Namman and Reinhardt 1995; EN 14561; Vandewalle 2000a, b);

b) CEB-FIP MC 2010 (2011), which also adopts the concept of residual flexural tensile strength parameters to derive the constitutive law that characterizes the tensile behavior of strain-softening and strain-hardening FRCs. The code proposes two simplified stress-crack width models based on the rigid-plasticity and linear-elasticity tensile behavior of FRCs. Correction factors are applied to scale the equivalent residual flexural strength at serviceability and ultimate limit states, which are determined from three-point bending tests conducted based on EN 14651 2007 (Blanco et.al 2013; Bakhshi et. al. 2013b);

c) German guidelines similar to RILEM (2003) for design of flexural members use the strain compatibility analysis to determine the flexural capacity of SFRC members (Teutsch 2004);

d) The United Kingdom (UK), which traditionally followed the Japan Concrete Institute test method JCI-SF4 (1984), but recently shifted toward the RILEM design methodology (Bar and Lee 2004) and methods based on EN 14651 (2007);

e) The Italian guidelines (di Prisco et al. 2006), which are based on load-crack tip opening displacements from 4-point bending tests on notched beams using equivalent stresses;

f) The Scandinavian approach, which is also based on residual strength parameters (Silfwerbrand 2008);

g) The United States, communicates research results primarily through ACI Committee 544 and the Fiber Reinforced Concrete Association (FRCA). The U. S. design guidelines for flexural members are based on empirical equations of Swamy et al. (1975), ASTM C1609 and C1399, Banthia and Dubey (1999, 2000), and Fischer (2004). The residual strength parameter is obtained using elastic section properties and effect of fiber type and concrete composition are not specified;

h) Soranakom and Mobasher (2007, 2008, 2009a) proposed closed form solutions to correlate the flexural load-deflection to a simplified tensile stress strain response—a procedure applicable to a wide variety of design applications, such as one- and two-way slabs, beams, slabs-on-ground, and earth retaining structures.

In a majority of these cases, the uniaxial compressive response is determined directly from standard compression cylinder tests. Flexural tests conducted by EN 14651 (2007) are recommended for characterization of tensile behavior. The CEB-FIP MC 2010 (2011) advises against using uniaxial tensile tests for standard testing of new mixtures due to the associated difficulty of execution and interpretation (Blanco et al. 2013). The long-term behavior of cracked FRC under tension, however, is required for those structural fibers, such as organic or natural fibers, whose long-term performance is influenced by creep. The CEB-FIP MC 2010 (2011) specifies if certain requirements about characteristic residual strengths and the limit of proportionality (LOP) (EN 14651 2007) are fulfilled, then fiber reinforcement can substitute conventional reinforcement at ultimate limit state (ULS).

CHAPTER 4—TEST METHODS

4.1—Test and specimen types

Various test methods exist for direct or indirect evaluation of the uniaxial-tensile properties of FRCs. These include uniaxial tensile, wedge splitting, and beam tests. Because beam tests are easier to implement in conventional field laboratories, the uniaxial-tensile properties of FRCs are often derived from these test data. Common flexural-beam tests are performed under a three- or four-point layout:

a) Three-point load recommended in RILEM (2003), CEB-FIP MC 2010 (2011), and ASTM C293;

b) Four-point load recommended in ASTM C78

c) Four-point load for FRC in ASTM C1399, ASTM C1609, DBV 1992 of the German Concrete Association, JCI-SF4 (1983) of the Japan Concrete Institute, and NBN B15-238-92, a Belgian Standard.

Beam tests can be subdivided by beam type:

a) Unnotched like those used by ASTM

b) Notched like those used with the three-point load test by RILEM 2003 and CEB-FIP MC 2010 (2011)

Controlling the post-peak response is much more dependable using a crack mouth opening displacement (CMOD) in a notched beam as opposed to deflection control used in unnotched beams. The CMOD measure in a notched beam is a monotonic increasing variable, which provides stable testing conditions while deflection includes elastic deformation outside the fracture process zone, which may cause unstable tests if extra caution is not considered (Hordijk

1991). Further detailed description of each beam type and test procedure is presented in the corresponding standards and, therefore, beyond the scope of this report.

4.2—Stress-strain diagrams

There are various ways to represent the load-carrying capacity of a sample after the point of maximum load. In each case the model should include the localization effect within the crack region where all incremental deformation is concentrated, while the remainder of the specimen undergoes unloading in an elastic or inelastic manner. Existing softening responses are subdivided into two main categories:

1) Stress–crack width definition
2) Stress-strain approach, where the strain is defined in terms of average displacement over a predetermined characteristic length or, alternatively, with a smeared crack approach (di Prisco 2004; CEB-FIP MC 2010 [2011])

The average strain over the descending response is affected by the definition of a characteristic length parameter as a material property, as crack opening is represented as a smeared crack.

4.3—Stress-strain diagram in the RILEM approach

The stress-strain diagram shown in Fig. 3.1 is proposed by RILEM (2003) and Vandewalle (2003). The values that define this constitutive model are based on a piecewise linearized response in the post peak domain. Average or characteristic values are then used later for design purposes.

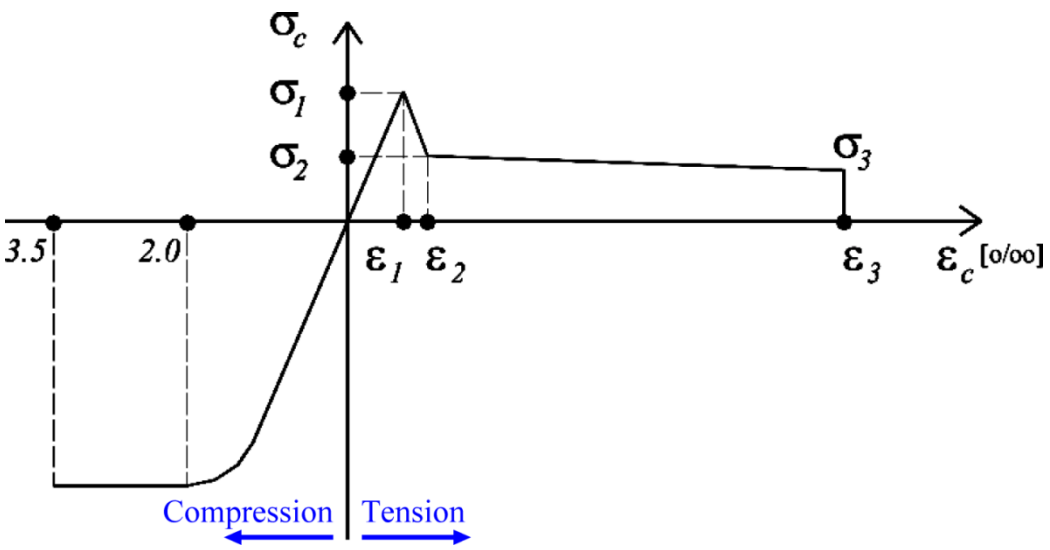

Fig. 4.3a—Stress–strain diagram for FRCs in uniaxial tension and compression (RILEM 2003; Vandewalle 2003).

In Fig. 4.3, the key points of the compression side of the diagram are taken directly from the standard compressive cylinder test. For the tension side of the diagram the key points are:

a) σ_1, and ε_1 – Tensile strength and corresponding strain;

b) σ_2, and ε_2 – Stress and strain at the onset of the stable strain-softening branch;

c) σ_3, and ε_3 – Stress and strain at the end of the softening branch.

The values of σ_i and ε_i (i=1,2,3) can next be directly related to beam test data using the approach presented in (Vandewalle 2000a, b; Vandewalle 2002a, b; Barros et. al. 2005). In this case σ_i (i=1,2,3) are related to the following characteristic points on the beam-test load displacement curve (Fig. 4.3b):

a) Average value of the flexural tensile strength, $f_{tm,fl}$, for example is, the limit of proportionality of the beam response;

b) Residual flexural tensile strength at deflection of 1/64 in. (0.46 mm), $f_{R,1}$;

c) Residual flexural tensile strength at deflection of 1/8 in. (3.0 mm), $f_{R,4}$.

Details on how to evaluate $f_{tm,fl}$, $f_{R,1}$ and $f_{R,4}$ are presented in 4.4 and details on the σ_i, ε_i, $f_{tm,fl}$, $f_{R,1}$ and $f_{R,4}$ are provided in 4.5.

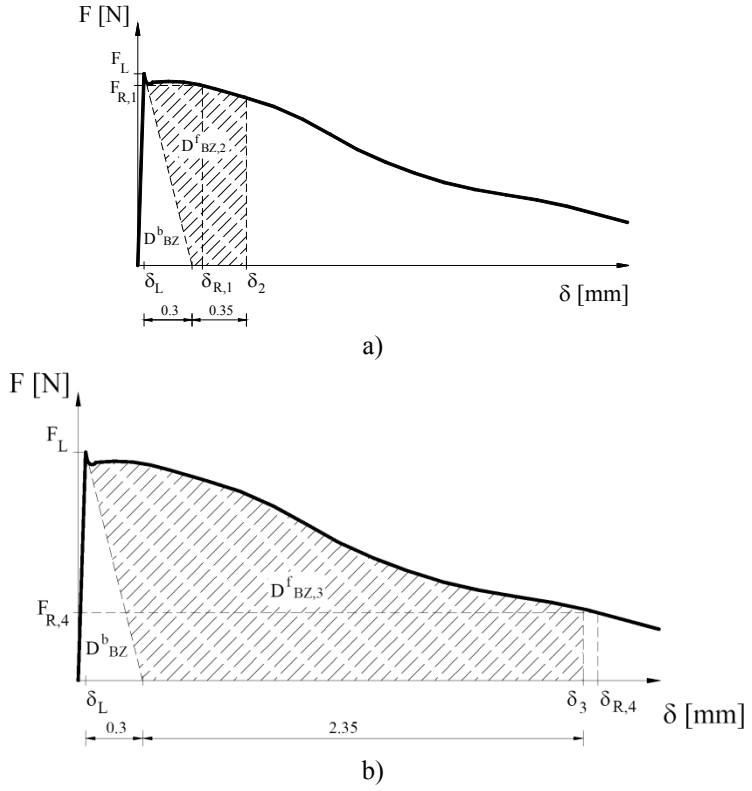

Fig. 4.3b—Load–displacement response of a test beam used to evaluate: a) $f_{R,1}$ from $F_{R,1}$ and b) $f_{R,4}$ from $F_{R,4}$ (Vandewalle 2000a, b; Vandewalle 2002a, b; Barros et al. 2005).

4.4—Flexural tensile strength, $f_{tm,fl}$, and residual flexural tensile strengths, $f_{R,1}$ and $f_{R,4}$

The flexural tensile strength, $f_{t,fl}$, and residual flexural tensile strengths, $f_{R,1}$ and $f_{R,4}$, values are calculated directly from the load displacement response of the test beam, which is schematically represented in Fig. 4.3b ($\delta_{R,1}$ = 1/64 in. (0.46 mm) and $\delta_{R,4}$ = (1/8 in. (3.0 mm)).

4.4.1 *Flexural tensile strength, $f_{t,fl}$ —*

The flexural tensile strength, $f_{t,fl}$, is defined as the maximum flexural tensile stress within the critical section at a load level equal to the limit of proportionality, F_L. The limit of

proportionality is the load at the end of the linear-elastic response, as shown in Fig. 4.3b. When there is no clear end point to the linear-elastic portion of the load-displacement curve, the limit of proportionality is defined as the highest load up to a deflection of 0.002 in. (0.05 mm) (Vandewalle et al. 2002a, b).

Similar to the modulus of rupture (MOR), f_r, of conventional concrete, the flexural tensile strength, $f_{t,fl}$, is calculated assuming linear stress distribution within the critical section. When a three-point beam bending test is used, variables L, and b define span and width of the test beam, h_n defines the net section height, and the flexural tensile strength, $f_{t,fl}$, is calculated as:

$$f_{t,fl} = \frac{3F_L L}{2bh_n^2} \qquad (4.4.1)$$

If a notched test beam is used, the net section height, h_n, equals the distance between the notch tip and cross-section top (h_{unc}). Alternatively, if the loading geometry changes from three-point bending to four-point bending, the parameters of the equation should be changed accordingly.

4.4.2 *Residual flexural strengths, $f_{R,1}$ and $f_{R,4}$*—

Residual flexural tensile strengths, $f_{R,1}$ and $f_{R,4}$, are taken from beam loads $F_{R,1}$ and $F_{R,4}$ that correspond to beam deflections of 1/64 in. (0.46) and 1/8 in. (3.0 mm), respectively (Vandewalle et al. 2002b), as shown in Fig. 4.3b. Although at this deflection level both (a) the stress distribution is no longer linear within the critical section, and (b) the uncracked beam height is smaller than its value at the limit of proportionality, h_{unc}, the same relationship to that used for calculating the flexural tensile strength, $f_{t,fl}$, is still used:

$$f_{R,1} = \frac{3F_{R,1}L}{2bh_{hunc}^2} \quad (4.4.2a)$$

$$f_{R,4} = \frac{3F_{R,4}L}{2bh_{hunc}^2} \quad (4.4.2b)$$

4.5—Relationship between uniaxial tensile stress and flexural strength

The flexural tensile strength, $f_{t,fl}$, and residual flexural tensile strengths, $f_{R,1}$ and $f_{R,4}$, can be directly related to the key tensile stress parameters σ_i (i=1,2,3) which define the stress-strain diagram shown in Fig. 4.3b. This relationship is a function of the specimen type and size, and introduced through stress coefficients C_1, C_2, C_3, values of which can be calculated from test data using an inverse analysis procedure.

4.6—Tensile stress-strain diagrams and strain values ε_1, ε_2, and ε_3

An inverse analysis procedure is used to determine the entire stress-strain response from the experimental tests. A more simple approach is to identify a few key points of the curve and use them to construct a piecewise response. Tensile strain value ε_1, is obtained following the Hooke's Law and using Young's modulus of FRC, E_c, which is assumed to be the same in compression and tension:

$$\varepsilon_1 = \frac{\sigma_1}{E_c} \quad (4.6)$$

Other strain values, ε_2, and ε_3 depend on the choice of modeling technique used for the back-calculation of the properties. A sample model is presented in the next section.

4.6.1 *Tensile stress values σ_1, σ_2, and σ_3*—

Relationships connecting tensile stress values, σ_i (i=1,2,3), with flexural-tensile values $f_{tm,fl}$, $f_{R,1}$ and $f_{R,4}$ vary depending on the type of test beam used:

1) Notched (RILEM 2003) three-point bending;

2) Belgian Standard NBN B15-238-92;

3) Unnotched ASTM C78 and ASTM C293;

4) Unnotched ASTM C1399 and ASTM C1609.

4.6.1.1 *RILEM notched three-point beam—*

If a notched (RILEM 2003) three-point bending is used, the specimen can be approximated as shown in Fig. 4.6.1.1.

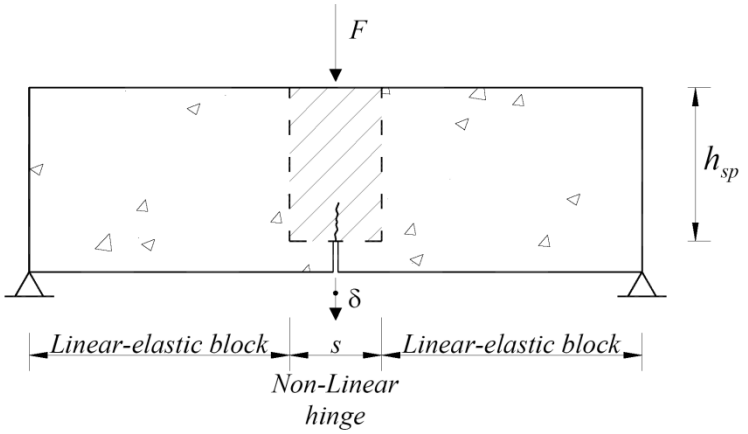

Fig. 4.6.1.1—Specimen idealization for model use (Barros et al. 2005). The uncracked section height, h_{unc}*, equals the distance between the notch tip and the cross section top,* h_{sp}.

Tensile stress values σ_1, σ_2, and σ_3, as defined in Fig. 4.3b, can now be calculated as:

$$\sigma_1 = C_1(1.6 - d) f_{tm,fl} \qquad (4.6.1.1a(a))$$

$$\sigma_2 = C_2 f_{R,1} \qquad (4.6.1.1a(b))$$

$$\sigma_2 = C_3 f_{R,4} \qquad (4.6.1.1a(c))$$

where d is the depth of the beam's cross section and $f_{tm,fl}$ is the average value of the flexural tensile strength, $f_{t,fl}$. In the original RILEM (2003) and Barros et al. (2005) there is a size factor k_h that is also introduced and the C_i stress coefficients and strain values can be assumed as (Barros et al. 2005):

$$C_1 = 0.52,\ C_2 = 0.36,\ C_3 = 0.27,\ \varepsilon_2 = 0.12\%,\ \varepsilon_3 = 10.4\% \qquad (4.6.1.1b)$$

4.6.1.2 *Belgian NBN unnotched four-point beam—*

Nemegeer-Harelbeke (1998) used the deformation-controlled bending test defined by Belgian Standard NBN B15-238-92 to evaluate FRC material properties. The test is a four-point bending test, with a span of 18 in. (457 mm), with beam width and height of 6 in. (150 mm).

Contrary to the approach presented above in which case loads are recorded at deflection of (1/64 in. (0.46 mm) and 1/8 in. (3.0 mm) [Barros et al. 2005], the Belgian Standard NBN B15-238 records loads at deflection of 1/16 in. (1.5 mm) and 1/8 in. (3 mm), for example, $F_{R\text{-}15}$ and $F_{R\text{-}30}$, respectively. Corresponding residual flexural strengths, $f_{R\text{-}15}$ and $f_{R\text{-}30}$, are calculated as:

$$f_{R\_15} = \frac{3F_{R-15}L}{2bh_n^2} \qquad (4.6.1.2a)$$

$$f_{R\_30} = \frac{3F_{R-30}L}{2bh_{unc}^2} \qquad (4.6.1.2b)$$

This approach is based on an equivalent elastic analysis and assumes that once a beam has cracked, the depth of the compressive zone can be estimated at about 10 percent of the beam height. The residual flexural tensile stress in the post-cracking range can be estimated as 37 percent of the corresponding linear-elastic stress. Resulting tensile stresses values σ_1, σ_2, and σ_3, as defined in Fig. 4.3a are:

$$\sigma_1 = 0.21MPa\left(\frac{f_c}{1MPa}\right)^{\frac{2}{3}} \qquad (4.6.1.2c)$$

$$\sigma_2 = 0.37 f_{R\_15} \qquad (4.6.1.2d)$$

$$\sigma_3 = 0.37 f_{R\_30} \qquad (4.6.1.2e)$$

$$\varepsilon_1 = \frac{\sigma_1}{E_c},\ \varepsilon_2 = 0.1\%\ \varepsilon_3 = 1\% \qquad (4.6.1.2f)$$

These strain values can be used to represent the serviceability and also the ultimate limit state. The C_i parameters and the strain values of the points that define the tensile behavior of a FRC can also be determined by inverse analysis using a FEM approach (Sena-Cruz et al. 2004; Mazaheripour et al. 2012), a cross section layer approach detailed in Barros and Sena-Cruz (2001), or an iterative procedure with a closed form solution, such as the one presented in Section 4 (Soranakom and Mobasher 2008). In the inverse analysis, the σ-ε tensile diagram is obtained by fitting, with the minimum error, the average force-deflection, or CMOD, curve recorded in the experimental notched beam bending tests.

4.6.1.3 *ASTM beam tests: ASTM C78 four-point, ASTM C293 three-point beams—*

ASTM C78 and ASTM C293 are used to obtain the flexural strength using unnotched third-point and center-point loading, respectively. These beam dimensions and general loading geometry have also been used within a different testing protocol to obtain the post-crack tensile response. Correlation of the ASTM test methods with the uniaxial stress-strain response of FRC indicates large fundamental differences such that no reported values for the stress coefficients C_1, C_2 and C_3 exist based on ultimate strength values from ASTM C78 and ASTM C293. No relationship exists that connects tensile stress values, σ_i (i=1,2,3), to load-displacement behavior of unnotched beams. An inverse analysis procedure that can be used to relate tensile stress values, σ_i (i=1,2,3), to load-displacement behavior of unnotched beams is described in Chapter 5.

4.6.1.4 *Unnotched ASTM C1399 and ASTM C1609 beams—*

The averaged residual strength (ARS), proposed by Banthia and Dubey (1999, 2000) is obtained through ASTM C1399 (1999), and ASTM C1609. ASTM C1399 (1999) is conducted by means of an open loop load controlled test machine on a precracked specimen. A steel plate is placed

underneath a concrete beam and the specimen is loaded under four-point bending until the concrete cracks. The purpose of using steel plate in the precracking process is so the load transferred onto the specimen does not diminish after cracking. The operator is expected to stop the precracking loading process immediately after the cracking begins. The steel plate is removed and the cracked specimen is reloaded for post-crack flexural loads at deflection levels of 0.02, 0.03, 0.04 and 0.05 in. (0.5, 0.75, 1.0, and 1.25 mm) for specimens 4 x 4 x 14 in. (100 x 100 x 350 mm). The equivalent stress results are averaged to represent ARS value. This parameter has been used as a method to compare different material formulations. Designers however, may erroneously use it as a tensile strength measure.

ASTM C1609 tests an unnotched specimen under deflection control to compute the post-peak flexural load-deflection response and utilizes a method similar to ARS proposed in ASTM C1399, where load-carrying capacity in the post-crack range is expressed as an equivalent stress measure. Figure 4.6.1.4 shows the set-up schematics for one of two linear variable differential transformers (LVDTs) used as closed loop feedback control parameters (ASTM C1609).

As the post-peak response is averaged, the residual load is used to calculate an elastically equivalent flexural stress using the section modulus of the uncracked beam where the moment is divided by the equivalent elastic section modulus. The problem with this test is that the formation of localized crack may vary within the third middle range of the specimen and the deflection control might not be an accurate measure of localization. Also during closed loop testing of unnotched specimens, support conditions in terms of friction, sliding, and rotational capacities become critical and can cause scatter in test results. Additionally the fixity of the roller

supports plays a dominant role in the results (Wille and Montesinos-Parra 2012). No reported values for the stress coefficients C_1, C_2 and C_3 exist based on ultimate strength values from ASTM C1399 and ASTM C1609. These issues pertaining to ASTM C1609 are being studied in ASTM committee C09.42.

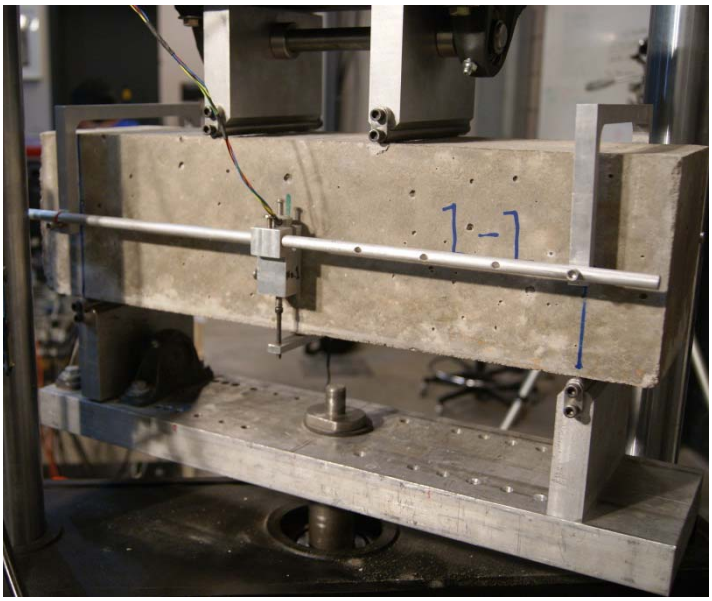

Fig. 4.6.1.4—Crack growth in FRC samples under four-point bending test (Mobasher et. al. 2011).

CHAPTER 5—STRESS-STRAIN CURVES BY BACK-CALCULATION APPROACH

5.1—Parametric stress-strain curves

A simplified stress-strain tensile model can be related to the flexural data using a closed-form solution of moment-curvature response and load-deflection calculation of fiber-reinforced concrete (FRC) as proposed by Soranakom and Mobasher (2007 a, b, c), Sonarakom et al. (2008). This approach relates the measured flexural load-deflection response of FRC test beams to tensile stress-strain response through an iterative process.

The constitutive model using nondimensional parameterized strain-softening and -hardening FRC is shown in Fig. 5.1a. The compression zone is linear elastic-perfectly-plastic (Fig. 5.1a(b) defined by a yield point (ε_{cy}, σ_{cy}) as it maintains at the constant yield stress σ_{cy} until the ultimate strain ε_{cu}.

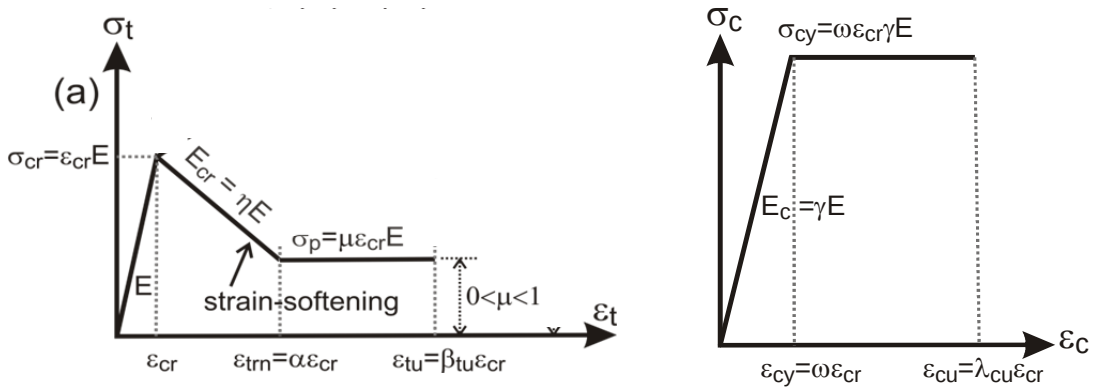

Fig. 5.1a—FRC model used by Soranakom and Mobasher (2007 a, b, c), Soranakom et. al. (2008), where (a) is tensile response and (b) is compression response.

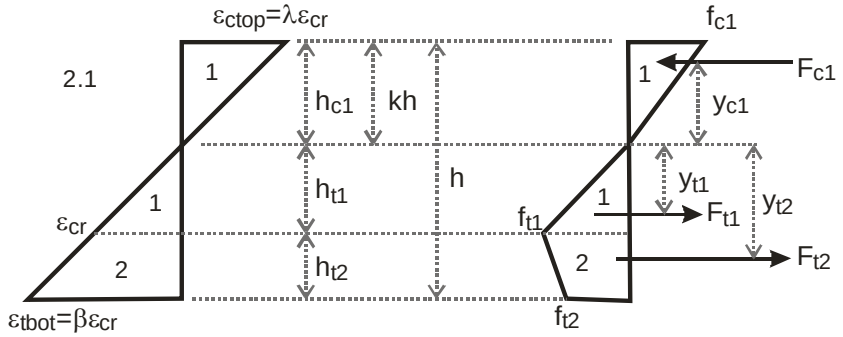

(a)

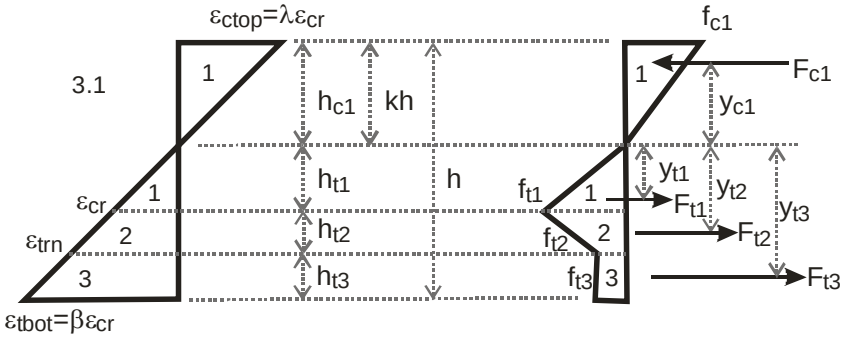

(b)

Fig. 5.1b—Strain and stress diagrams at the post crack stage where (a) is strain distribution and (b) is stress distribution (Soranakom and Mobasher (2007 a, b, c)). (Refer to Stages 2.1 and 3.1 in Table 4 for post crack stage.)

The tension strain ε_t is described by a nondimensional strain measure β, and using a piecewise linear response with an elastic range E, up to the tensile strength point, ε_{cr} and followed by a residual tensile strength, μ as shown in Fig. 5.1a(a). Three strain measures define the first cracking (ε_{cr}), transition strain (ε_{trn}), and the ultimate tensile strain level (ε_{tu}). Ultimate tensile and compressive strains limit the flexural strength capacity. With this approach, all strains and stresses are normalized in terms of the cracking strain ε_{cr}, and cracking strength $\sigma_{cr}=\varepsilon_{cr} E$. Corresponding normalized strain parameters α, β, β_{tu}, ω, λ, and λ_{cu}, as well as stress parameter μ are defined in Fig. 5.1a and Eq. 5.1a. The ultimate tensile strain level β_{tu} is used as the limiting

state, while first cracking tensile strain ε_{cr} and tensile modulus E are used as intrinsic material parameters to normalize other parameters:

$$\omega = \frac{\varepsilon_{cy}}{\varepsilon_{cr}}; \quad \alpha = \frac{\varepsilon_{trn}}{\varepsilon_{cr}}; \; \beta = \frac{\varepsilon_t}{\varepsilon_{cr}}; \quad \beta_{tu} = \frac{\varepsilon_{tu}}{\varepsilon_{cr}}; \; \lambda_{cu} = \frac{\varepsilon_{cu}}{\varepsilon_{cr}}; \quad \mu = \frac{\sigma_p}{E\varepsilon_{cr}} \tag{5.1a}$$

Nomenclature used is:

a) Cracking strength in tension σ_{cr} defined as $\varepsilon_{cr}E$;

b) Post-cracking strength in tension, defined using scalar parameter μ, $\sigma_p = \mu\varepsilon_{cr}E$;

c) Transition point in the post-crack strain in tension, defined using scalar parameter α, $\varepsilon_{trn} = \alpha\varepsilon_{cr}$;

d) Yield strength in compression $\sigma_{cy} = \omega\varepsilon_{cr}E$;

e) Yield strain in compression $\varepsilon_{cy} = \omega\varepsilon_{cr}$;

f) Limit state ultimate tensile strain ε_{tu} defined using scalar parameter β_{tu}, $\varepsilon_{tu} = \beta_{tu}\varepsilon_{cr}$;

g) Limit state ultimate compressive strain $\varepsilon_{cu} = \lambda_{cu}\,\varepsilon_{cr}$.

h)

A relationship has been proposed between the approach by Soranakom and Mobasher (2007 a, b, c) and the approach by EN 14651:

$$\sigma_1 = \sigma_{cr}$$
$$\sigma_2 = \sigma_3 = \sigma_P \tag{5.1b}$$
$$\varepsilon_1 = \varepsilon_2 = \varepsilon_{cr}$$
$$\varepsilon_3 = \varepsilon_{tu}$$

Refer to Appendix A for a discussion of the procedure to calculate the closed form moment curvature and load-deflection curve. This strategy is extended to FRC elements that can also include longitudinally steel- and fiber-reinforced polymer bars, where ε_2 can be higher than ε_1, and σ_p higher than σ_{cr} to simulate strain-hardening FRCs (Mobasher 2011; Taheri et al. 2011).

5.2—Back-calculation of flexural test data

Figure 5.2 presents the back-calculated tensile stress-stain response and flexural load-deflection response of macro synthetic fibers (Bakhsi et al. 2013). The effect of curing time on the tensile data is obtained from the flexural load-deflection results and plotted in Fig. 5.2(a). The initial tensile response is linear elastic up to about 0.6, 1.2 and 1.6 MPa for 8, 16 and 36 h samples as the first crack stage. After cracking, the load is transferred to the fibers, and crack bridging results in strain-softening response. Back-calculated tensile stress-strain responses show that after an average strain level of about 0.0025 mm/mm, the residual strength of the macro synthetic fiber composites reaches a constant value. The post-crack residual strength at this plateau zone increases from about 0.35 to 0.55 and 0.7 MPa due to aging from 8 to 16 and 36 h. A maximum curvature versus deflection plot is also shown in Fig. 5.2(a) and represents a linear response. As shown in Fig. 5.2(b), the simulated response for the load-deflection response shows a good correlation with the experimental data. The parameter μ representing the normalized post-crack strength of the materials is obtained as 0.52, 0.44, and 0.46, respectively for 8, 16, and 36 h cured samples. Note that all these samples are classified as strain softening with parameter μ defined as the normalized post-crack residual tensile strength.

The sudden drop in moment capacity after cracking refers to deflection-softening response. According to the model by Soranakom and Mobasher (2008, 2009b), assuming that there is only a single segment to the softening response (for example, α=1), the transition from deflection softening to deflection hardening takes place at a critical post-crack tensile strength of:

$$\mu_{crit} = \frac{\omega}{3\omega - 1} \tag{5.2}$$

The critical post crack tensile strength level μ_{crit} that maintains a load-carrying capacity equivalent to the cracked strength level. A value of $\mu_{crit} = 0.35$ is obtained at a compressive strength to tensile strength ratio ω=9, and characterizes two subclasses of materials—deflection softening ($\mu < 0.35$) and deflection hardening ($\mu > 0.35$).

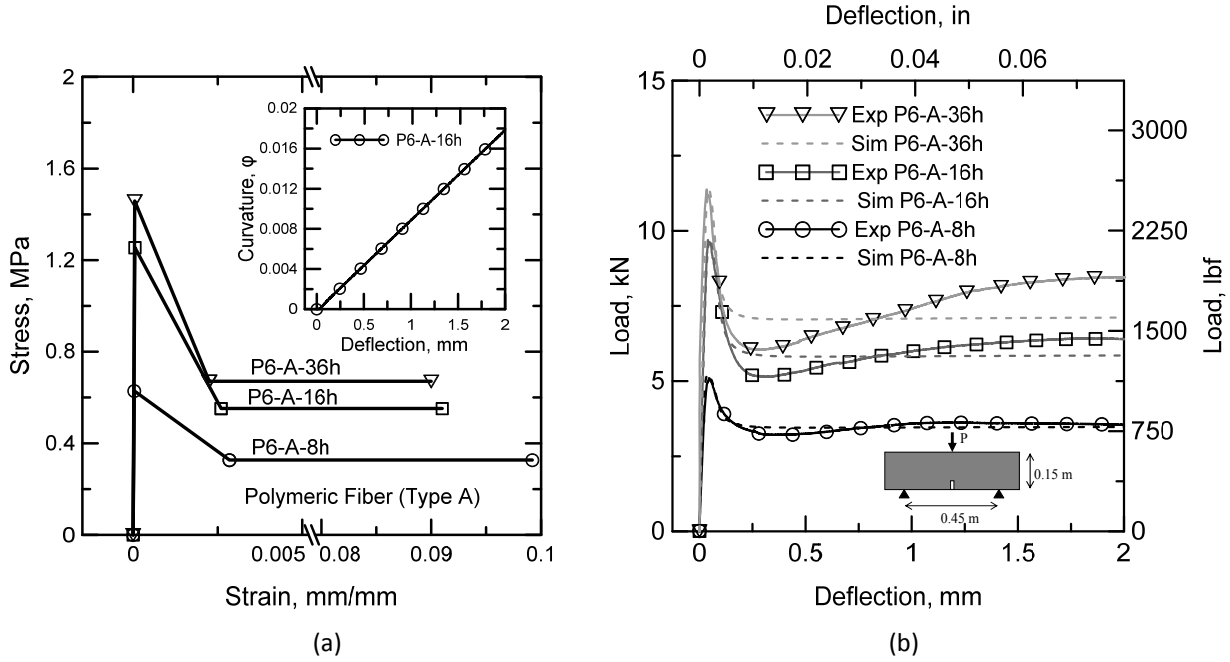

Fig. 5.2—(a) Effect of age on back-calculated tensile stress-strain response, and a representative curvature-deflection relationship, (b) effect of age on experimental and simulated load-deflection response for polymeric fibers (Bakhshi et. al. 2013b).

5.3—Comparison with averaged residual strength (ARS) results

ASTM C1399; and ASTM C1609 can be used by means of spreadsheet-based inverse analysis procedures (Soranakom and Mobasher 2007 a, b, c). Correlation of residual strength from ASTM C1609 and the back-calculated method is addressed next. To illustrate the differences in the interpretation of test data between an equivalent elastic and strain-softening approach, the stress distribution during the late stage of a macro fiber sample composite is presented across the cross sectional depth in Fig. 5.3 (Soranakom and Mobasher 2010). Using a strain-softening

material model captures the incremental movement of the neutral axis, magnitude of compressive stress, and residual tensile stress. The simulation of Fig. 5.3 on polypropylene FRC reveals a discrepancy between the present method and ARS, in accordance to ASTM C1399 or ASTM C1609, which is primarily due to a difference in stress distribution between the two test methods (Mobasher 2011).

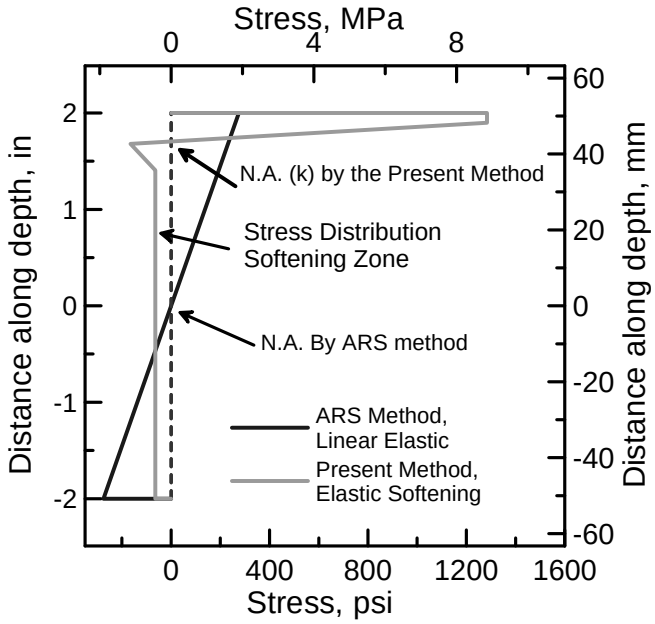

Fig. 5.3—Comparison of stress distribution in the present back-calculation approach with the ARS method (Soranakom and Mobasher [2010]; Bakhshi et al. [2013a]).

Note that specimen size effect has considerable influence on the measured residual flexural strength parameters; for example, ASTM C1399 currently only allows the testing of 4 x 4 x 14 in. (100 x 100 x 350 mm) sized beams. ASTM C1609, however, allows the use of both 4 x 4 x 14 in. (100 x 100 x 350 mm) and 6 x 6 x 20 in. (150 x 150 x 500 mm) specimen sizes, depending on the length of the constituent fibers. Size effect causes smaller beam sizes to show higher residual flexural strength parameters.

5.4—Comparison with RILEM and JCI methods

Similar comparisons of back-calculation data can be made with equivalent models obtained from the RILEM method as well. Results indicate the linear elastic based residual strength approaches overestimate the residual tensile strength by as much as 300 percent. The inconsistency is in residual strength calculation using linear elastic approach; the neutral axis is assumed fixed at the centroid and the stress distribution is linear, leading to nominal flexural stress levels which are far greater than tensile strength. Based on this inconsistency, engineers should exercise extreme caution when applying the ARS method in design and analysis of FRC sections. Although discussions of the ASTM C1609 test method are beyond the scope of this report, note that the ARS value is not an equivalently elastic stress and, therefore, is marginally associated with post-crack tensile strength or tensile residual strength parameter σ_p as defined in Fig. 5.1a. JCI-SF4 (1986) recommends calculating an equivalent flexural strength from flexural toughness and specimen geometry. The *Soranakom and Mobasher* approach requires an adjustment factor of 1/3.11=0.32 and 1/3.2=0.31 as shown in Fig. 5.4, which correlates extremely well with the recommended values by RILEM (2003), JCI-SF4 (1986), and Barros et al. (2005) for a variety of mixture formulations (Bakhshi et al. 2013a).

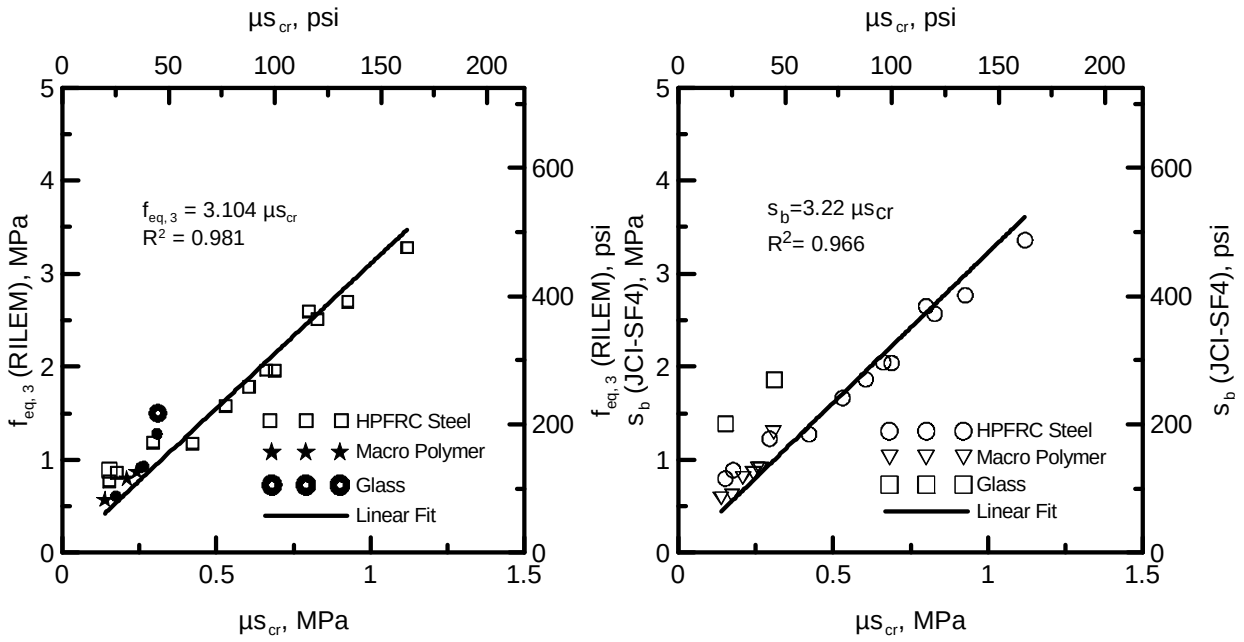

Fig. 5.4—Correlation of residual strength from the ASTM C1609 and Soranakom and Mobasher (2010) approach requires an adjustment factor of 3.1-3.2.

CHAPTER 6—REFERENCES

ACI committee documents and documents published by other organizations are listed first by document number and year of publication followed by authored documents listed alphabetically.

Standards
ASTM International

C78/C78M-10 Standard Test Method for Flexural Strength of Concrete (Using Simple Beam with Third-Point Loading)

C293/C293M-10 Test Method for Flexural Strength of Concrete (Using Simple Beam with Center-Point Loading)

C1399/C1399M-10 Test Method for Obtaining Average Residual-Strength of Fiber-Reinforced Concrete

C1609/C1609M-12	Test Method for Flexural Performance of Fiber-Reinforced Concrete (Using Beam With Third-Point Loading)
Belgian standards	
NBN B15-238-92	Tests on Fibre Reinforced Concrete – Bending Test on Prismatic Samples (Available only in Dutch and French)
British Standards Institute (BSI)	
EN 14651:2005+A1:(2007)	Test Method for Metallic Fibre Concrete. Measuring the Flexural Tensile Strength (Limit of Proportionality (LOP), residual)
DBV (German Concrete Association)	
DBV 1992	Design Principles of Steel Fibre-Reinforced Concrete for Tunneling Works
European standards	
CSN EN 14561-07	Chemical disinfectants and antiseptics - Quantitative carrier test for the evaluation of bactericidal activity for instruments used in the medical area - Test method and requirements (phase 2, step 2)
Japan Concrete Institute	
JCI-SF4-83	Methods of Tests for Flexural Strength and Flexural Toughness of Fiber Reinforced Concrete
Authored documents	

Barr B., and Lee, M. K., 2004, "FRC Guidelines in the UK, with Emphasis on SFRC in Floor Slabs," *Proceeding of the North American/European Workshop on Advances in Fiber Reinforced Concrete*, *BEFIB 2004,* Bergamo, Italy, Sept., pp. 29-38.

Bakhshi, M.; Laungrungrong, B.; Bonakdar, A.; Mobasher, B.; Borror, C. M.; Montgomery, D. C., 2013a, "Economical Concrete Mix Design Utilizing Blended Cements, Performance-Based Specifications, and Pay Factors," FHWA-AZ-13-633, Final Report 633, May, 111 pp.

Bakhshi, M.; Barsby, C.; Mobasher, B., 2013b,"Comparative Evaluation of Early Age Toughness Parameters in Fiber Reinforced Concrete," *Materials and Structures*, DOI 10.1617/s11527-013-0098-1.

Banthia, N., and Dubey, A., 1999, A. "Measurement of Flexural Toughness of Fiber-Reinforced Concrete Using a Novel Technique - Part 1: Assessment and Calibration," *ACI Materials Journal*, V. 96, No. 6, Dec., pp. 651-656.

Banthia, N. and Trottier, J. F., 1995a, "Test Methods for Flexural Toughness Characterization of Fiber Reinforced Concrete: Some Concerns and a Proposition," *ACI Materials Journal*, V. 92, No. 1, Jan., pp. 48-57.

Banthia, N. and Trottier, J. F., 1995b "Concrete Reinforced with Deformed Steel Fibres, Part II: Toughness Characterization" *ACI Materials Journal,* V. 92, No. 2, Mar., pp. 146-154.

Barros, J. A. O.; Cunha, V. M. C. F.; Ribeiro, A. F.; and Antunes, J. A. B., 2005, "Post-cracking Behaviour of Steel Fibre Reinforced Concrete (RILEM Recommendations)," RILEM *Materials and Structures*, V. 38, No. 1, Jan.-Feb., pp. 47-56.

Barros, J. A. O., and Sena-Cruz, J. M., 2001, "Fracture Energy of Steel Fibre Reinforced Concrete," *Journal of Mechanics of Composite Materials and Structures,* V. 8, No. 1, Jan.–Mar., pp. 29-45.

Blanco, A.; Pujadas, P.; de la Fuente, A.; Cavalaro, S.; Aguado, A., 2013, "Application of Constitutive Models in European Codes to RC-FRC," *Construction and Building Materials*, V. 40, Mar., pp. 246-259.

British Standard Institute, 2007, "Test Method for Metallic Fibered Concrete–Measuring the Flexural Tensile Strength (Limit of Proportionality (LOP), Residual), BS EN 14651:*2005+A1:2007*, Osterreichisches Normunqsinstitut Publications, an ASI Global Service, Paramus, NJ, Dec., 18 pp. (Published in German).*CEB-FIBP (Comite Euro-International du Beton-International Federation for Structural Concrete),* 2011, "fib Model Code for Concrete Structures 2010 (MC 2010), Model Code prepared by Special Activity Group 5 (SAG5), Lausanne, Switzerland, Oct., 434 pp.

Cunha, V. M. C. F., 2010, "Steel Fibre Reinforced Self-Compacting Concrete: From Micro-Mechanics to Composite Behaviour," PhD Thesis, University of Minho, 467 pp.

di Prisco, M.; Toniolo, G.; Plizzari, G. A.; Cangiano, S.; and Failla, C., 2004, "Italian Guidelines on SFRC in Fiber-Reinforced Concrete: From Theory to Practice," *Proceeding of the North American/European Workshop on Advances in Fiber Reinforced Concrete*, *BEFIB 2004,* Bergamo, Italy, Sept., pp. 39-72.

Fischer, G., 2004, "Current U.S. Guidelines on Fiber Reinforced Concrete and Implementation in Structural Design," *Proceeding of the North American/European Workshop on Advances in Fiber Reinforced Concrete*, *BEFIB 2004,* Bergamo, Italy, Sept., pp.13-22.

Hordijk, D.A., 1991, "Local Approach to Fatigue of Concrete," Dissertation, Delft University of Technology, pp. 216.

Mazaheripour, H.; Barros, J. A. O.; Soltanzadeh, F.; Gonçalves, D. M. F., 2012, "Interfacial Bond Behaviour of GFRP Bar in Self-Compacting Fiber Reinforced concrete", 8th RILEM International Symposium on Fibre Reinforced Concrete: challenges and opportunities, Eds: Joaquim Barros et al., Sept., pp. 12.

Mobasher, B., 2011, "Mechanics of Fiber and Textile Reinforced Cement Composites," First ed., CRC Press; Boca Raton, FL, 450 pp.

Mobasher, B.; Krauss, S.; Dey, V.; Barsby, C.; Bakhshi, M.; Bonakdar, A., 2011, "Flexural Testing of MasterFiber™ MAC Matrix Reinforced Concrete," Report to BASF – The Chemical Company, 31 pp.

Naaman, A. E., and Reinhardt, H. W., 2005, "Proposed Classification of HPFRC Composites Based on Their Tensile Response," *Construction Materials*, *Proceedings of the 3rd International Conference on Construction Materials: Performance, Innovations and Structural Implications - ConMat '05 and Mindess Symposium*, The University of British Columbia, Aug., 170 pp.

Naaman, A. E., and Reinhardt, H. W., 2006, "Proposed Classification of FRC Composites Based on Their Tensile Responses," *Material Structure*, V. 39, No. 5, pp. 547-555.

Nemegeer-Harelbeke, D., 1998, Design Guidelines for Dramix Steel Fibre-Reinforced Concrete, Bekaert.

Noghabai, K., 1998, “Effect of Tension Softening on the Performance of Concrete Computational Studies,” PhD Thesis, Dept. of Civil and Mining Eng., Division of Structural Eng., Lülea University of Technology, Sweden, pp. 458.

RILEM, 2003,Technical Committee TC 162-TDF 1995 (2003), “Final Recommendations of RILEM TC 162-TDF: Test and Design Methods for Steel Fibre Reinforced Concrete,” *Materials and Structures*, V. 36, No. 36, Oct., pp. 560-567.

Sena-Cruz, J. M.; Barros, J. A. O.; Ribeiro, A. F.; Azevedo, A. F. M.; Camões, A. F. F. L., 2004 "Stress-Crack Opening Relationship of Enhanced Performance Concrete," 9th Portuguese Conference on Fracture, ESTSetúbal, Portugal, Feb. 18-20, pp. 395-403.

Silfwerbrand, J., 2008, “Codes for SFRC Structures – A Swedish Proposal,” Tailor Made Concrete Structures – Walraven & Stoelhorst (eds.), pp. 553-558.

Soranakom, C., and Mobasher, B., 2007a, “Closed-Form Moment-Curvature Expressions For Homogenized Fiber Reinforced Concrete,” *ACI Materials Journal*, V. 104, No. 4, July-Aug.

Soranakom, C. and Mobasher, B., 2007b, “Flexural Modeling of Strain Softening C Strain Hardening Fiber Reinforced Concrete,” H.W. Reinhardt and A.E. Naaman, Co-editors, *"High Performance Fiber Reinforced Cement Composites - HPFRCC 5,"* RILEM Proceedings, Pro. 53, S. A R. L., Cachan, France, pp.155-164.

Soranakom, C., and Mobasher, B., 2007c, “Closed Form Solutions for Flexural Response of Fiber Reinforced Concrete Beams” *ASCE Journal of Engineering Mechanics*, V. 133, No. 8., Aug., 8 pp.

Soranakom, C., and Mobasher, B., 2008, "Moment-Curvature Response of Strain Softening and Strain Hardening Cement Based Composites," *Cement and Concrete Composites,* V. 30, No. 6, July, pp. 465-477.

Soronakom, C., and Mobasher B., 2009a, "Design Flexural Analysis and Design of Textile Reinforced Concrete," *Textile Reinforced Structures: Proceedings of the 4nd Colloquium on Textile Reinforced Structures (CTRS4) und zur 1. Anwendertagung, SFB 528*, Technische Universität Dresden, Eigenverlag, – ISBN 978-3-86780-122-5, pp. 273-288.

Soranakom, C., and Mobasher, B., 2009b, "Flexural Design of Fiber Reinforced Concrete," *ACI Materials* Journal, Sept.-Oct., pp. 461-469.

Soronakom, C., and Mobasher B., 2010, "Flexural Analysis and Design of Strain Softening Fiber Reinforced Concrete," *ACI Proceedings*, ACI-SP-272, Eds., G. J. Para-Montesinos, P. Balaguru, pp. 173-187.

Soranakom, C.; Yekani-Fard, M.; and Mobasher, B., 2008, "Development of Design Guidelines For Strain Softening Fiber Reinforced Concrete," *7th International Symposium of Fiber Reinforced Concrete: Design and Applications BEFIB*, Ed. R. Gettu, Sept., pp. 513-523.

Swamy, R. N.; Mangat, P. S.; and Rao, C. V. S. K., 1975, "The Mechanics of Fiber Reinforced Cement Matrices," *Fiber Reinforced Concrete ACI SP-44*, pp. 1-28.

Taheri, M.; Barros, J. A. O.; Salehian, H. R., 2011, "A Design Model for Strain-Softening and Strain-Hardening Fiber Reinforced Elements Reinforced Longitudinally with Steel and FRP Bars," *Composites - Part B Journal*, V. 42, pp. 1630-1640.

Teutsch, M., "German Guidelines on Steel Fiber Concrete," *Proceeding of the North American/European Workshop on Advances in Fiber Reinforced Concrete*, *BEFIB 2004,* Bergamo, Italy, Sept. 2004, pp. 23-28.

Van Mier, J., 1996, Fracture Processes of Concrete: Assessment of Material Parameters for Fracture Models, CRC Press, Dec., 464 pp.

Vandewalle, L., 2000a, "Test and Design Methods for Steel Fiber Reinforced Concrete – Recommendations for Bending Tests," *Materials and Structures*, V. 33, No. 225, Jan.-Feb. pp. 3-5.

Vandewalle, L., 2000b, "Test and Design Methods for Steel Fiber Reinforced Concrete Recommendations for σ-ε Design Method," *Materials and Structures,* V. 33, No. 226, Mar., pp. 75-81.

Vanderwalle, L., 2002a, "Design of Steel Fibre Reinforced Concrete Using σ-w Method: Principles and Applications," *Materials and Structures Journal*, June, V. 35, No. 5, pp. 262-278.

Vandewalle, L., 2002b, Test and Design Methods for Steel Fiber Reinforced Concrete – Final Recommendation," *Materials and Structures*, V. 35, No. 253, Nov., pp. 579 - 582.

Vandewalle, L., 2003, Test and Design Methods for Steel Fiber Reinforced Concrete – s-e Design Method – Final Recommendation," *Materials and Structures*, V. 36, No. 262, Oct., pp. 560–567.

Wille, K., Montesinos-Parra, J. G., 2012, "Effect of Beam Size, Casting Method, and Support Conditions on Flexural Behavior of Ultra-High-Performance Fiber-Reinforced Concrete," *ACI Materials Journal*, V. 109, No. 3, May-June, pp. 379-388.

APPENDIX A—SPREADSHEET-BASED INVERSE ANALYSIS PROCEDURES

This report presents existing methods for estimating uniaxial stress-strain response of strain-softening fiber-reinforced concretes (FRC) using beam test data. Methods are based on an inverse analysis of beam data experimentally validated. Appendix A.1 presents: (a) a complete spreadsheet-based inverse analysis for center- or third-point loaded test beams; and (b) specific relationships for specific beam types (RILEM 2003). Relationships can be used for other beam types by determining stress coefficients C_1, C_2, and C_3 using one of the described inverse analysis methods.

A.1—Simplified strain-softening/hardening FRC model

For the inverse analysis procedure, a general strain hardening tensile and an elastic perfectly plastic compression model as derived by Soranakom and Mobasher (2007a, b, c; 2008, 2009b) is shown in Fig. A.1. Tensile response is the defined by tensile stiffness, E, first crack tensile strain ε_{cr}, cracking tensile strength, σ_{cr}, $=E\varepsilon_{cr}$, ultimate tensile capacity, ε_{peak}, and post crack modulus E_{cr}. The softening range is shown as a constant stress level $\mu E\varepsilon_{cr}$. The compression response is defined by the compressive strength σ_{cy} defined as $\omega\gamma E\varepsilon_{cr}$. To simplify material characteristics of strain-hardening FRC and generate closed form design equations, classical assumptions, such as plane section remain plane, linear strain distribution, small deformations, are made. By ignoring the post-peak ranges in both and compression, the closed-form equations can be simplified further to the idealized bilinear tension and elastic compression models as shown in Fig. A.1(a) and (b). To reduce the complexity of material response to the useable range, disregard the post-peak tensile response and plasticity in the compression region. It has been shown that the difference in compressive and tensile modulus has negligible effect to the ultimate moment capacity (Soranakom and Mobasher 2008). By defining all parameters as

normalized, with respect to minimum number of variables, closed-form derivations are obtained. Applied tensile and compressive strains at bottom and top fibers, β, and λ are defined as

$$\beta = \frac{\varepsilon_t}{\varepsilon_{cr}},\ \lambda = \frac{\varepsilon_c}{\varepsilon_{cr}} \tag{A.1a}$$

Material parameters required for the simplified models are summarized as follows. Parameters, α, μ, η, ω, are defined respectively as representing normalized, tensile strain at peak strength, post-crack modulus, and compressive yield strain:

$$\alpha = \frac{\varepsilon_{peak}}{\varepsilon_{cr}},\ \eta = \frac{E_{cr}}{E},\ \omega = \frac{\sigma_{cy}}{E\varepsilon_{cr}} = \frac{\sigma_{cy}}{\sigma_{cr}} \tag{A.1b}$$

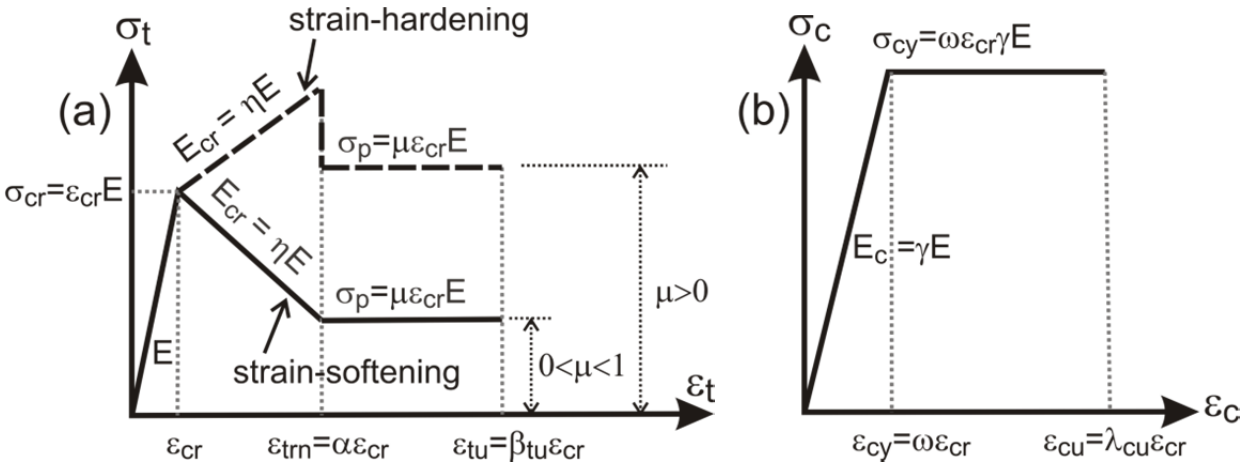

Fig. A.1—Full option material models for both strain-hardening and strain-softening FRC: (a) compression model; and (b) tension model.

A.2—Derivation of the moment-curvature diagram

For typical strain-hardening FRC, the compressive strength is higher than the tensile strength. Thus, flexural capacity is controlled by the weaker tension and compressive stress is normally low in the elastic range. For this reason, the elastic compression model (Fig. A.2(b)) is used. For the development of design equations, the accompanying compressive stress developed in a beam

section is limited to the yield compressive stress $\sigma_{cy} = 0.85 f_c'$ at compressive yield strain ε_{cy}, where f_c' is the uniaxial compressive strength.

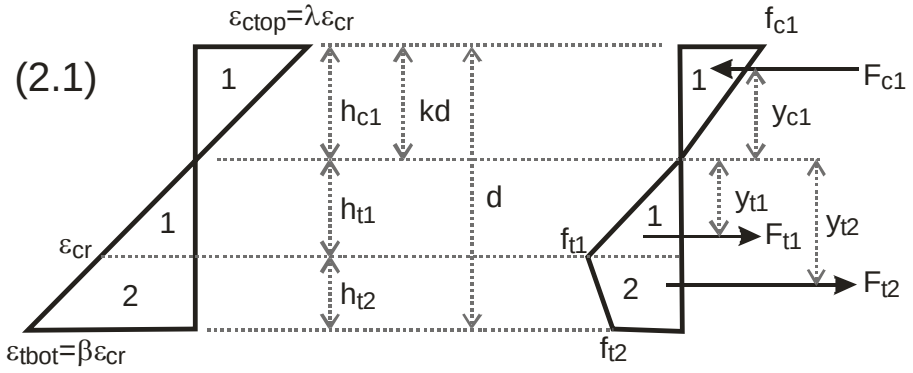

(a) Strain distribution (b) Stress distribution

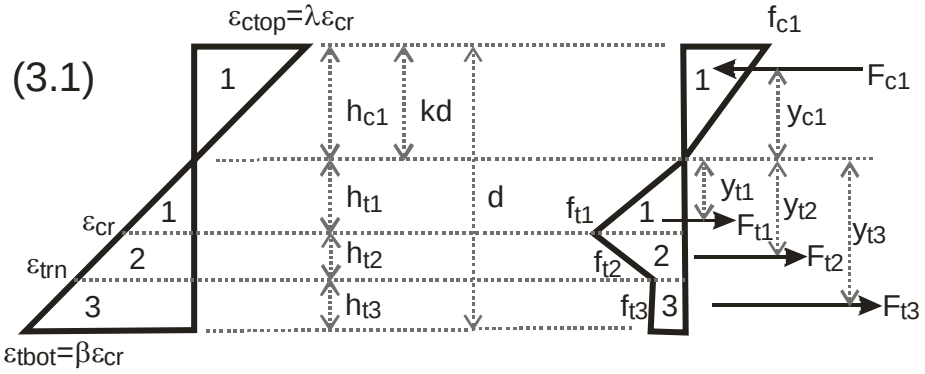

(a) Strain distribution (b) Stress distribution

Fig. A.2— Strain and stress diagrams at the post-crack stage (Ranges 2.1 and 3.1 in Table A.1).

Table A.1—Neutral axis parameter k, normalized moment m and normalized curvature ϕ for each stage of normalized tensile strain at bottom fiber (β).

Stage	K	m = M/M$_{cr}$	$\phi = \Phi/\ \Phi_{cr}$
1 $0 < \beta \leq 1$	$k_1 = \begin{cases} \frac{1}{2} & \text{for } \gamma=1 \\ \frac{-1+\sqrt{\gamma}}{-1+\gamma} & \text{for } \gamma \neq 1 \end{cases}$	$m_1 = \frac{2\beta\left[(\gamma-1)k_1^3 + 3k_1^2 - 3k_1 + 1\right]}{1-k_1}$	$\phi'_1 = \frac{\beta}{2(1-k_1)}$
2.1 $1 < \beta \leq \alpha$ $0 < \lambda \leq \omega$	$k_{21} = \frac{D_{21} - \sqrt{D_{21}\gamma\beta^2}}{D_{21} - \gamma\beta^2}$ $D_{21} = \eta\left(\beta^2 - 2\beta + 1\right) + 2\beta - 1$	$M'_{21} = \frac{\left(2\gamma\beta^3 - C_{21}\right)k_{21}^3 + 3C_{21}k_{21}^2 - 3C_{21}k_{21} + C_{21}}{1-k_{21}}$ $C_{21} = \frac{(2\beta^3 - 3\beta^2 + 1)\eta + 3\beta^2 - 1}{\beta^2}$	$\phi'_{21} = \frac{\beta}{2(1-k_{21})}$
3.1 $\alpha < \beta \leq \beta_{tu}$ $0 < \lambda \leq \omega$	$k_{31} = \frac{D_{31} - \sqrt{D_{31}\gamma\beta^2}}{D_{31} - \gamma\beta^2}$ $D_{31} = \eta\left(\alpha^2 - 2\alpha + 1\right)$ $+ 2\mu(\beta - \alpha) + 2\alpha - 1$	$M'_{31} = \frac{\left(2\gamma\beta^3 - C_{31}\right)k_{31}^3 + 3C_{31}k_{31}^2 - 3C_{31}k_{31} + C_{31}}{1-k_{31}}$ $C_{31} = \frac{(2\alpha^3 - 3\alpha^2 + 1)\eta - 3\mu\left(\alpha^2 - \beta^2\right) + 3\alpha^2 - 1}{\beta^2}$	$\phi'_{31} = \frac{\beta}{2(1-k_{31})}$

A.3—Derivation of moment capacity

Moment capacity of a beam section, according to the imposed tensile strain at the bottom fiber ($\varepsilon_t = \beta\varepsilon_{cr}$), can be derived based on the assumed linear strain distribution as shown in Fig. A.1(a). By using material models described in Fig. A.1(a) and (b), the corresponding stress diagram is obtained as shown in Fig. A.2(b) in which the stress distribution is subdivided into a compression zone 1, and tension zones 1 and 2. Force components and their centroidal distance to the neutral axis in each zone can be expressed as:

$$\frac{F_{c1}}{bh\sigma_{cr}} = \frac{\beta\gamma k^2}{2(1-k)}; \qquad \frac{y_{c1}}{h} = \frac{2}{3}k \tag{A.3a}$$

$$\frac{F_{t1}}{bh\sigma_{cr}} = \frac{(1-k)}{2\beta}; \qquad \frac{y_{t1}}{h} = \frac{2}{3}\frac{(1-k)}{\beta} \tag{A.3b}$$

$$\frac{F_{t2}}{bh\sigma_{cr}} = \frac{(1-k)(\beta-1)(\eta\beta-\eta+2)}{2\beta}; \qquad \frac{y_{t2}}{h} = \frac{2\eta\beta^2-\eta\beta-\eta+3\beta+3}{3\beta(\eta\beta-\eta+2)}(1-k) \quad \text{(A.3c)}$$

where F and y are the force and its centroid, respectively; subscripts *c1,t1,t2* designate compression zone 1, tension zone 1 and 2, respectively; b and h are the width and the height of the beam, respectively. The neutral axis parameter k is found by solving the equilibrium of net internal forces equal to zero, $F_{c1} + F_{t1} + F_{t2} = 0$.

$$k = \frac{C_1 - \sqrt{\beta^2 C_1}}{C_1 - \beta^2}; \text{ where } C_1 = \eta\left(\beta^2 - 2\beta + 1\right) + 2\beta - 1 \quad \text{(A.3d)}$$

The nominal moment capacity M_n is obtained by taking the first moment of force about the neutral axis, $M_n = F_{c1}y_{c1} + F_{t1}y_{t1} + F_{t2}y_{t2}$, and express it as a product of the normalized nominal moment m_n and the cracking moment M_{cr} as follows in Eq. (A.3e) and (A.3f):

$$M_n = m_n M_{cr} \quad , \quad M_{cr} = \frac{\sigma_{cr} bh^2}{6} \quad \text{(A.3e)}$$

$$m_n = C_2 \frac{k^2 - 2k + 1}{\beta^2} + \frac{2\beta k^3}{1-k}; \text{ where } C_2 = C_1 + 2C_1\beta - \beta^2 \quad \text{(A.3f)}$$

If the full stress strain response is desired, then the location of neutral axis and moment capacity are obtained under the definitions provided in Table A.1. In this table the derivations of all potential combinations for the interaction of tensile and compressive response are presented. Analysis of these equations indicates that the contribution of fibers is mostly apparent in the post-cracking tensile region, where the response continues to increase after cracking (Fig. A.1(a)). The post-crack modulus E_{cr} is relatively flat with values of η= 0.00-0.4 for a majority of cement composites. The tensile strain at peak strength ε_{peak} is relatively large compared to the cracking tensile strain ε_{cr}, and may be as high as α = 100 for polymeric-based fiber systems. These unique characteristics cause the flexural strength to continue increasing after cracking.

Since typical strain-hardening FRC does not have significant post-peak tensile strength, the flexural strength drops after passing the tensile strain at peak strength. Also, the effect of post-crack tensile response parameter μ can be ignored for a simplified analysis. Determine the simplest parameters in terms of post-crack stiffness η and post-crack ultimate strain capacity α to estimate the maximum moment capacity for the design purposes.

According to bilinear tension and elastic compression models shown in Fig. A.1(a) and Fig. A.1(b), the maximum moment capacity is obtained when the normalized tensile strain at the bottom fiber ($\beta = \varepsilon_t/\varepsilon_{cr}$) reaches the tensile strain at peak strength ($\alpha = \varepsilon_{peak}/\varepsilon_{cr}$). However, the simplified equations, Eq. (A.3f) to (A.3h) for moment capacity, are applicable for the compressive stress in elastic region only. The elastic condition should be checked by computing the normalized compressive strain developed at the top fiber λ and compared to the normalized yield compressive strain ω. The general solutions for all the cases are presented in Table A.1. Use the strain diagram in Fig. A.2(a) to find the relationship between the top compressive strain and bottom tensile strain as follows:

$$\frac{\varepsilon_c}{kh} = \frac{\varepsilon_t}{(1-k)h} \tag{A.3g}$$

By substituting $\varepsilon_c = \lambda\varepsilon_{cr}$ and $\varepsilon_t = \beta\varepsilon_{cr}$ in Eq. (A.4), then limit the maximum compressive strain to the yield compressive strain $\varepsilon_{cy} = \omega\varepsilon_{cr}$. Finally, the condition can be expressed in a normalized form as:

$$\lambda = \frac{k}{1-k}\beta \quad \leq \quad \omega \tag{A.3h}$$

The case represented by case 2.1 of Table A.1, where the tensile behavior is in elastic-plastic while the compressive behavior is still elastic, is studied in this section. Equations for other

cases can also be developed. The general solution presented in Table A.1 can be simplified as follows:

The location of neutral axis represented as a function of applied tensile strain β is represented as (Eq. (A.3i)):

$$k = \frac{\sqrt{A}}{\sqrt{A} + \beta\sqrt{\gamma}} \qquad A = \eta(\beta^2 + 1 - 2\beta) + 2\beta - 1 \tag{A.3i}$$

This equation can be easily simplified by assuming equal tension and compression stiffness (γ=1). For an elastic perfectly plastic tension material (η=0), the equation reduces to (Eq. (A.3j)) :

$$k = \frac{\sqrt{2\beta - 1}}{\sqrt{2\beta - 1} + \beta} \tag{A.3j}$$

Table A.3 presents the case of (γ=1), for different values of post-crack stiffness η = 0.5, 0.2, 0.1, 0.05, 0.01, and 0.001. Note that the neutral axis is a function β and can be used in calculation of the moment, or the moment curvature relationship. These general responses, which are shown in Fig. A.3(a) and (b), show that with an increase in applied tensile strain, the neutral axis compression zone decreases. Note, however, that this decrease is a function of a post-crack tensile stiffness factor. Although the moment curvature relationship in this range is ascending, its rate is a function of the post-crack tensile stiffness. The parameter-based fit equations in the third and fourth column are obtained by curve fitting the simulated response from the closed-form derivations and are applicable within one percent accuracy of the closed-form results. Using these equations, the moment capacity and moment-curvature response can be generated for any cross section using basic tensile material parameters in the 2.1 range as defined in Table A.3.

Table A.3—Location of Neutral axis, moment, and moment-curvature response of a strain hardening composite material with γ = 1 η= 0.0001- 0.5

η	A, $(k=\frac{\sqrt{A}}{\sqrt{A}+\beta})$	$M'(k)$	$M'(\varphi)$
0.5	$0.5(\beta^2+1-2\beta)+2\beta-1$	$-0.773+0.108x10^{-1}k^{-6}$	$0.507+0.686\varphi$
0.2	$0.2(\beta^2+1-2\beta)+2\beta-1$	$0.654+0.516x10^{-2}k^{-6}$	$1.105+0.383\varphi$
0.1	$0.1(\beta^2+1-2\beta)+2\beta-1$	$1.276+0.289x10^{-2}k^{-6}$	$1.461+.234\varphi$
0.05	$0.05(\beta^2+1-2\beta)+2\beta-1$	$1.645+.1632x10^{-2}k^{-6}$	$1.720+.1401\varphi$
0.01	$0.01(\beta^2+1-2\beta)+2\beta-1$	$0.852+0.456\,k^{-1}$	$1.342+0.371\sqrt{\varphi}$
0.0001	$0.0001(\beta^2+1-2\beta)+2\beta-1$	$3.177-3.068\,k$	$3.021-2.047/\sqrt{\varphi}$

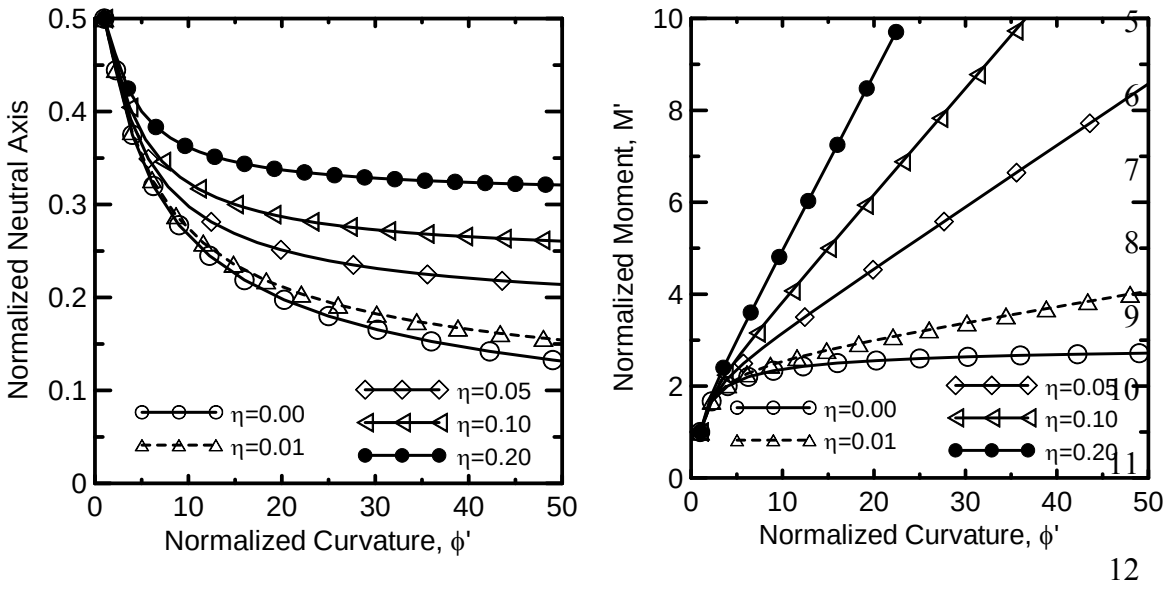

(a) (b)

Fig. A.3—Effect of (a) depth of neutral axis on the moment capacity of a section, and (b) the moment curvature response in the range 2.1.

A.4—Simplified moment curvature diagram

Figure A.3(b) shows the simplification of normalized moment curvature diagrams to normalized bilinear moment curvature diagrams for deflection hardening and deflection softening. In the simplified models, the intersection points (ϕ'_{it}, M'_{it}) of the linear elastic response and the linear post-crack response is found by using a regression Eq. (A.4). The regression equation is dimensionless and independent of the unit used.

$$M'_{it} = 0.7425M'_{u} + 0.1739 \qquad and \quad \phi'_{it} = M'_{it} \tag{A.4}$$

A.5—Load-deflection response

Figure A.5(a) shows the set up for three- and four-point bending tests. Figure A.5(b) show moment distributions at cracking and ultimate levels. With the area moment method, the corresponding curvature diagrams shown in Fig. A.5(c) to A.5(e) are divided into several areas and taken around the left support to obtain the midspan deflection δ. A set of equations for calculating midspan deflection of three-point bending at first bilinear cracking, at ultimate strength when material has $\mu > \mu_{crit}$, and at ultimate strength when material has $\mu < \mu_{crit}$ are presented in Eq. (A.5a) to Eq. (A.5c).

$$\delta_{bcr} = \frac{1}{12} L^2 \phi_{bcr} \tag{A.5a}$$

$$\delta_u = \frac{L^2}{24M_u^2}\left[\left(2M_u^2 - M_u M_{bcr} - M_{bcr}^2\right)\phi_u + \left(M_u^2 + M_u M_{bcr}\right)\phi_{bcr}\right] \qquad \mu > \mu_{crit} \tag{A.5b}$$

$$\delta_u = \frac{\phi_u L_p}{8}\left(2L - L_p\right) + \frac{M_u \phi_{bcr} L}{12M_{bcr}}\left(L - 2L_p\right) \qquad \mu < \mu_{crit} \tag{A.5c}$$

Similarly, a set of equations for four-point bending can be written as:

$$\delta_{bcr} = \frac{23}{216} L^2 \phi_{bcr} \tag{A.5c}$$

$$\delta_u = \frac{L^2}{216M_u^2}\left[\left(23M_u^2 - 4M_uM_{bcr} - 4M_{bcr}^2\right)\phi_u + \left(4M_u^2 + 4M_uM_{bcr}\right)\phi_{bcr}\right] \qquad \mu > \mu_{crit} \qquad \text{(A.5d)}$$

$$\delta_u = \frac{5L^2\phi_u}{72} + \frac{M_uL^2\phi_{bcr}}{27M_{bcr}} \qquad \mu < \mu_{crit} \qquad \text{(A.5e)}$$

Load step P_i can be back-calculated from a discrete point i along the moment curvature diagram:

$$P_i = \frac{2M_i}{S} \qquad \text{for } \phi_i = 0...\phi_u \qquad \text{(A.5f)}$$

where S is a spacing between the support and loading point, $S=L/2$ for three-point bending and $S=L/3$ for four-point bending.

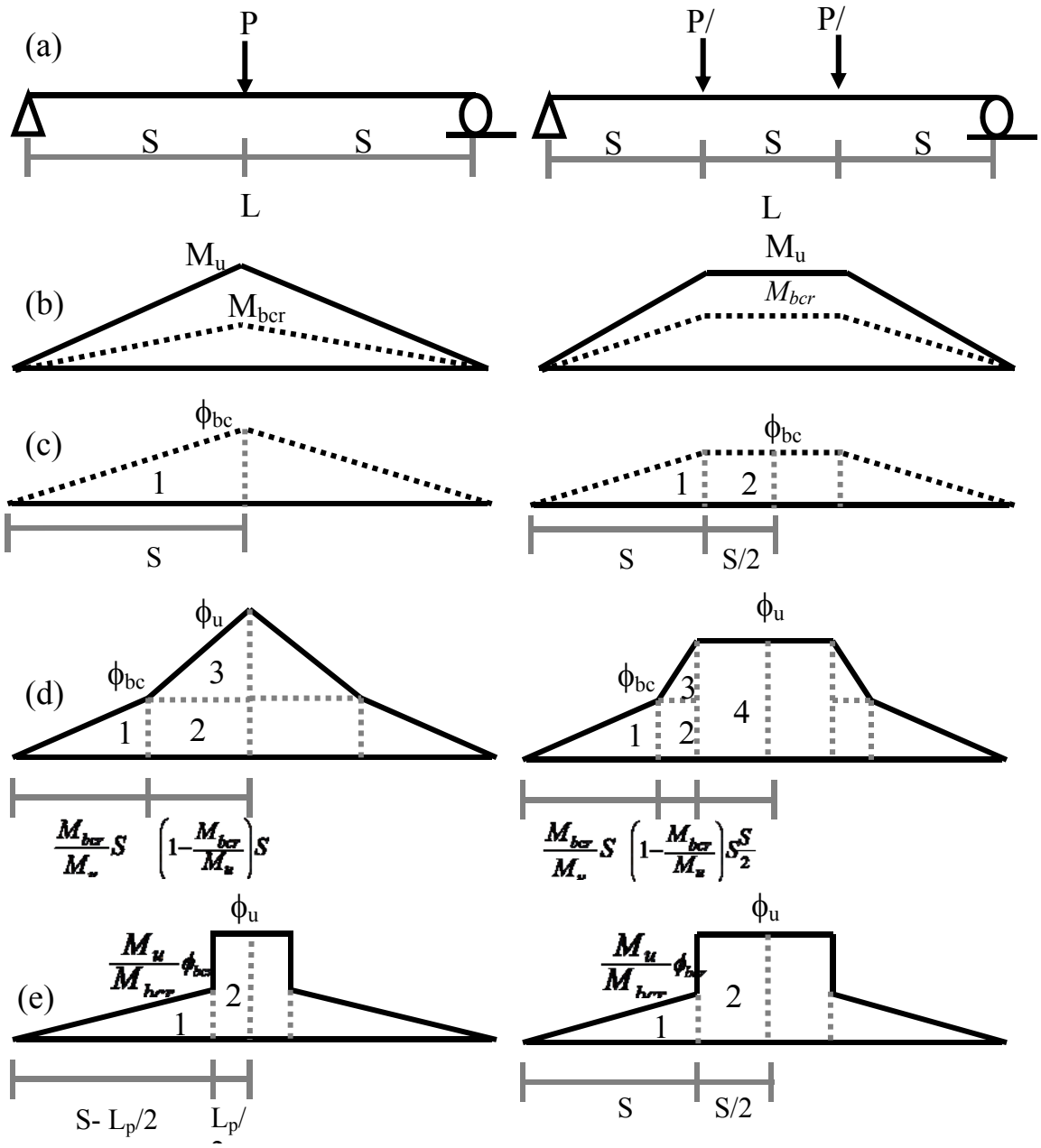

Fig. A.5—Three- and four-point bending test: (a) Experimental setup; (b) Moment distribution; (c) Curvature distribution at first bilinear cracking; (d) Curvature distribution at ultimate moment for high normalized post peak tensile strength ($\mu > \mu_{crit}$); (e) Curvature distribution at ultimate moment for low normalized post peak tensile strength ($\mu < \mu_{crit}$).

A.6—Example: Three-point bending test

Determine the moment curvature diagram and load deflection response of a beam size 4 x 4 in. (100 x 100) mm tested under three-point bending at clear span L = 12 in. (300 mm). Assume the plastic length for crack localized zone under the point load L_p 4 in. = (100 mm). The ultimate uniaxial compressive strength f'_c= 4300 psi (30 MPa), uniaxial tensile strength σ_{cr} = 360 psi (2.50 MPa), and post-peak tensile strength σ_p = 100 psi (0.75 MPa). The ultimate compressive strain ε_{cu} = 0.003 and the ultimate tensile strain ε_{tu} = 0.02.

The Young's modulus equals E = 3,600,000 psi (25,000 MPa).

Using the specified material properties, determine the normalized material parameters.

(assuming no nonlinear response, (α=1, and η=1) These parameters are calculated as:

Cracking strain: $\varepsilon_{cr} = \sigma_{cr}/E$ = 2.5/25000 = 0.0001

Normalized post peak tensile strength: $\mu = \sigma_p/\sigma_{cr}$ = 0.75/2.5 = 0.30

Normalized ultimate tensile strain: $\beta_{tu} = \varepsilon_{tu}/\varepsilon_{cr}$ = 0.02/0.0001 = 200

Normalized ultimate compressive strain: $\lambda_{cu} = \varepsilon_{cu}/\varepsilon_{cr}$ = 0.003/0.0001 = 30

Assumed compressive yield stress: $\sigma_{cy} = 0.8*fc'$ = 0.8*30 = 24 MPa

Compressive to tensile strain ratio: $\omega = \sigma_{cy}/(E\varepsilon_{cr})$ = 24/2.5 = 9.6

Using the parameters computed above, and input parameters such as *test method* = 3 (three-point bending) or 4 (four-point bending), b = 4 in. (100 mm), d = 4 in. (100 mm), L = 12 in. (300 mm), L_p = 4 in. (100 mm), E = 3,600,000 (25,000 MPa).

According to the material parameters input, tensile and compressive stress-strain responses are calculated. The critical normalized post-peak tensile strength μ_{crit}=0.345 is calculated by Eq. (A.6a).

$$\mu_{crit} = \frac{\omega}{3\omega - 1} = \frac{9.6}{3(9.6) - 1} = 0.345 \quad \text{(A.6a)}$$

Since $\mu = 0.30 < \mu_{crit}$, the worksheet shows Type 2 (deflection softening in accordance with definitions of Naaman and Reinhardt 2005). According to the normalized ultimate tensile failure β_{tu}, the corresponding normalized top compressive strain λ_{tu} is checked, which shows that the compressive strain fail at stage 3 ($\omega < \lambda$).

$$\beta_{tu} = 200 > \frac{\left(\omega^2 + 2\mu - 1\right)}{2\mu} = \frac{\left(9.6^2 + 2*0.3 - 1\right)}{2*0.3} = 152.9 \quad \text{(A.6b)}$$

$\lambda_{tu} < \lambda_{cu}$ means that the ultimate tensile strain will reach the failure before the compressive strain crushing. The smaller of λ_{tu} (=11.03) and λ_{cu} *(=30)* is used as a normalized ultimate compressive strain λ_u in the calculation of neutral axis depth ratio k_u by Eq. (A.6c).

$$k_u = \frac{2\mu\lambda}{-\omega^2 + 2\lambda(\omega + \mu) + 2\mu - 1} = 0.052 \quad \text{(A.6c)}$$

$$M'(\lambda, k, \omega, \mu) = \frac{(3\mu\lambda^2 + 3\omega\lambda^2 - 3\mu - \omega^3 + 2)k^2}{\lambda^2} - 3\mu(2k - 1) = 0.868 \quad \text{(A.6d)}$$

$$\phi'(\lambda, k, \omega, \mu) = \frac{\lambda}{2k} = \frac{11.03}{2(0.052)} = 105.52 \quad \text{(A.6e)}$$

The normalized ultimate moment M'_u and curvature ϕ'_u are calculated by Eq. (A.6d) and (A.6e), respectively as 0.868, and 105.52. The intersection points (ϕ'_{it}, M'_{it}) of the linear elastic and the linear post-crack response for bilinear moment curvature diagram is found by regression Eq. (A.12). The normalized cracking moment curvature always equal to one, ($\phi'_{cr} = M'_{cr} = 1$).

Because the material is deflection softening, the normalized reduced cracking moment M'_{cr2} is needed and calculated by Eq. (A6.f) as 0.818.

$$\phi'_{it} = M'_{it} = 0.7425M'_{u} + 0.1739 \quad = 0.7425(0.868) + 0.1739 = 0.818 \qquad \text{(A.6f)}$$

The four controlling points for normalized moment and curvature and dimensionalized moment and curvature, in addition to the computed load and deflection values for these control points, are obtained as shown in Table A.6a.

Table A.6a—Normalized and dimensionalized moment and curvature with computed load and deflection values

ϕ'	M'		ϕ, mm^{-1}	M, N.mm		δ, mm	P, N
0.000	0.000		0.000E+00	0		0.0000	0
1.000	1.000		2.000E-06	416,667		0.0150	5,556
1.000	0.818		2.000E-06	340,929		0.0150	4,546
105.521	0.868		2.110E-04	361,528		1.3234	4,820

The moment curvature response is recovered by multiplying the cracking moment curvature to their normalized moment curvature using equations in Table A.1. The deflections of three-point bending for the deflection softening $\mu<\mu_{crit}$ are calculated (Eq. (A.5b), (A.5c)) and the load calculated (Eq. (A.5f)). Note that the deflections at the cracking are the same but the load step due to M_{bcr} and M_{cr2} are different.

Alternatively, the accurate moment curvature diagram is found using equations listed in Table A.1. Figure A.5 compares the accurate moment curvature diagram and their approximate bilinear models. The load deflection response, according to bilinear models, is shown in Fig. A.6a. For

the four-point bending test, the procedure is similar, except L_p is not needed; users can enter any value or simply zero. An accurate expression for moment curvature can be developed using the closed-form equations identifying each of the three zones of response (Table A.6b).

Table A.6b—Diagram of accurate moment curvature

Accurate moment curvature diagram						
Stage	λ	k	ϕ'	M'	ϕ	M
1	0.00	0.500	0.000	0.000	0.00E+00	0
1	1.00	0.500	1.000	1.000	2.00E-06	416,667
2	1.86	0.267	3.480	0.772	6.96E-06	321,519
2	3.15	0.166	9.510	0.802	1.90E-05	334,339
2	5.30	0.103	25.725	0.837	5.15E-05	348,761
2	7.45	0.075	49.644	0.854	9.93E-05	355,836
2	9.60	0.059	81.267	0.864	1.63E-04	359,936
3	9.97	0.057	87.334	0.865	1.75E-04	360,432
3	10.34	0.055	93.401	0.866	1.87E-04	360,835
3	10.70	0.054	99.468	0.867	1.99E-04	361,166
3	11.07	0.052	105.535	0.867	2.11E-04	361,442

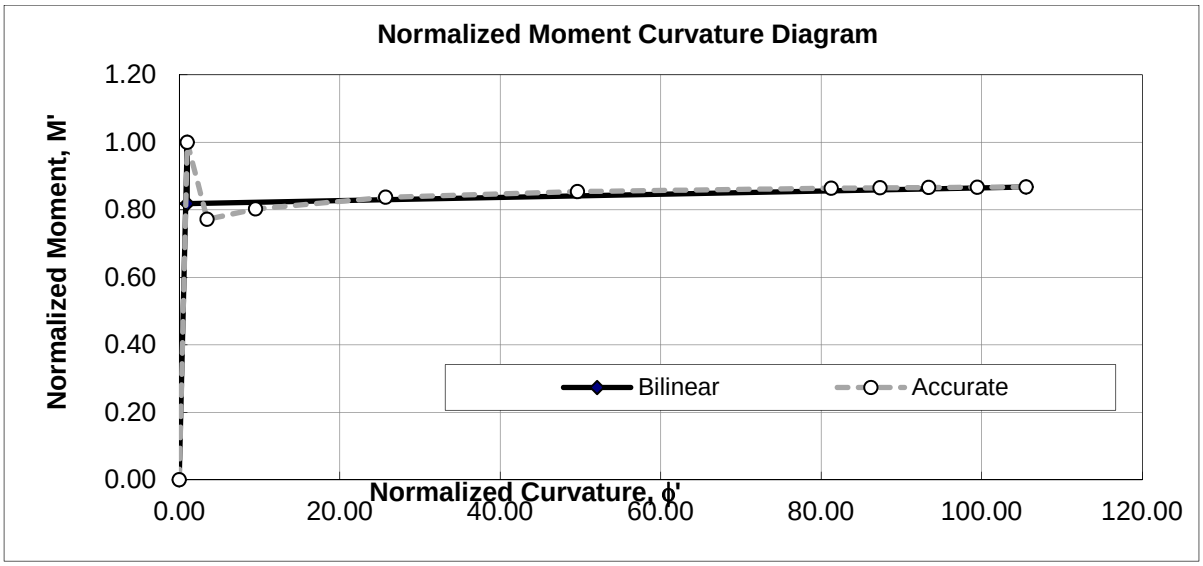

(a)

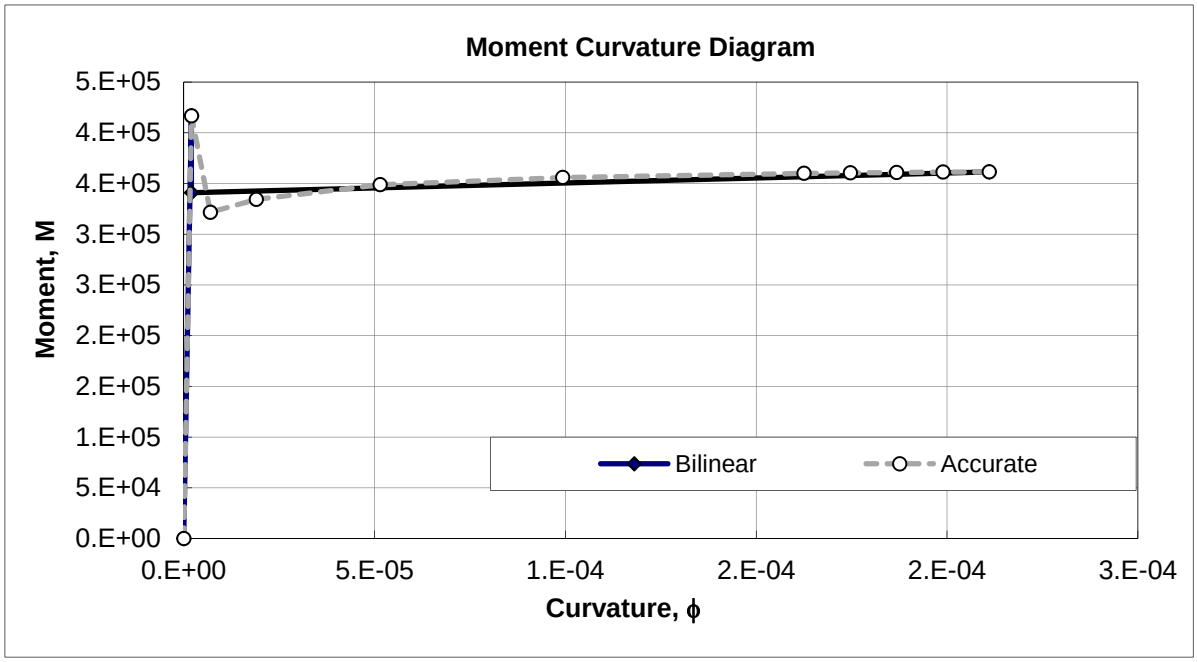

(b)

Fig. A.6a—(a) Normalized moment-curvature response and (b) its corresponding dimensionalized moment-response using the simplified and exact procedures for a rectangular cross section.

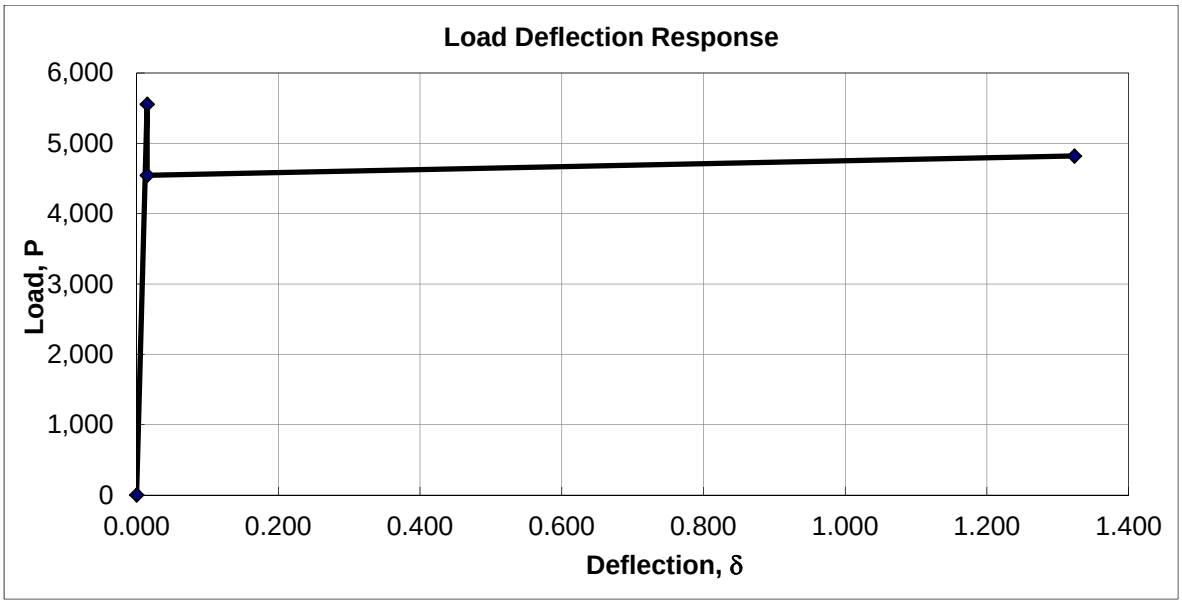

Fig. A.6b—Computed load and deflection values for the example case of a beam presented in TableA.6a.